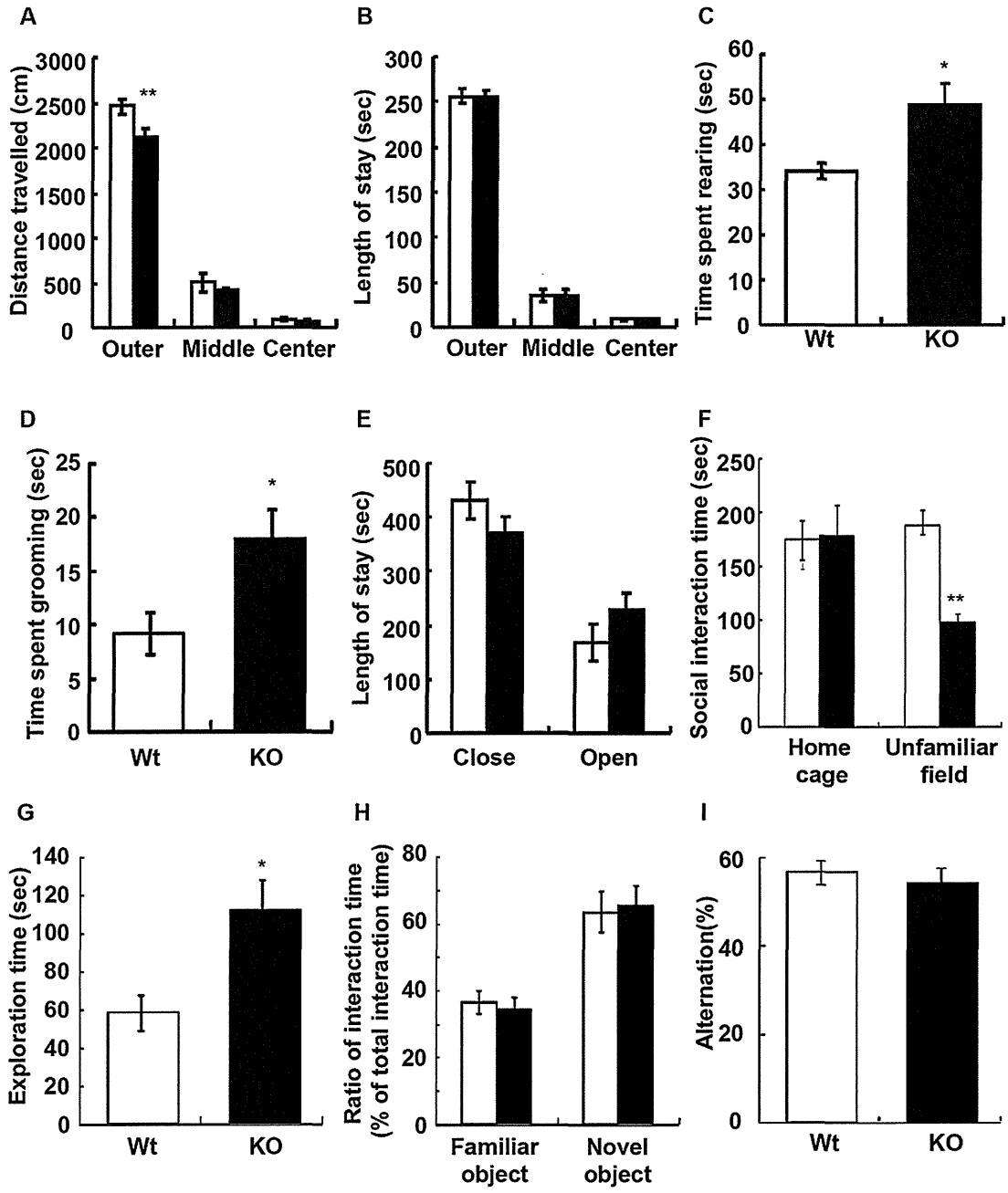

Fig. 3. Spontaneous behavior of *Shati*-knockout mice. Behaviors of *Shati*-knockout mice (KO, black column) were compared with those of wild type mice (Wt, white column). In the open field, distance traveled (A), length of stay in each area (B), rearing frequency (C) and grooming time (D) among the spontaneous behaviors of KO mice over the observation time of 5 min were compared with those of Wt mice. Results are presented as the mean ± S.E. $n = 8$ Wt mice (male = 5 and female = 3) and $n = 9$ KO mice (male = 5 and female = 4). (A) $^{**}p < 0.01$ KO vs. Wt. (C and D) $^{*}p < 0.05$ KO vs. Wt by Student's *t*-test. (E) Data from the elevated plus maze in KO mice (closed column) were compared with those in Wt mice (open column). The mice were placed in the elevated plus maze for 10 min. Results are presented as the mean ± S.E. $n = 8$ Wt mice (male = 5 and female = 3) and $n = 10$ KO mice (male = 5 and female = 5). (F) Social interaction time in the home cage or unfamiliar field during the observation period of 10 min. Results are presented as the mean ± S.E. $n = 8$ Wt mice (male = 5 and female = 3) and $n = 10$ KO mice (male = 5 and female = 5). $^{**}p < 0.01$ KO vs. Wt mice in unfamiliar field by Bonferroni's post tests. (G) Exploration time of objects in the acquisition phase of the novel object recognition test. Results are presented as the mean ± S.E. $n = 8$ Wt mice (male = 5 and female = 3) and $n = 10$ KO mice (male = 5 and female = 5), $^{*}p < 0.05$ vs. Wt, Student's *t*-test. (H) Ratio of interaction time between familiar object and novel object in the retention phase of the novel object recognition test. Results are presented as the mean ± S.E. $n = 8$ Wt mice (male = 5 and female = 3) and $n = 10$ KO mice (male = 5 and female = 5). (I) Ratio of correct entry in Y-maze test. Results are presented as the mean ± S.E. $n = 8$ Wt mice (male = 5 and female = 3) and $n = 10$ KO mice (male = 5 and female = 5).

with a novel mouse in an unfamiliar environment compared with the wild type mice in the social interaction test. Interestingly, the interaction time of *Shati*-knockout mice with intruder mice in their home cage was same as that of wild type mice. *Shati*-knockout mice interacted normally with their littermates in the home cage. The reason for the reduction in social interaction time of *Shati*-knockout mice in the unfamiliar environment is not clear, although the exploration time of a novel object was increased. These results suggest that absence of SHATI in the knockout mice resulted in social anxiety in stressful circumstances. Since GDNF plays an important role in social interactions [17], the remarkable reduction of GDNF expression in *Shati*-knockout mice may induce impairment of social interaction. Moreover, Uchida et al. [17] suggested that reduction of GDNF plays crucial roles in the behavioral responses of mice to chronic stress. In the *Shati*-knockout mice, reduction of GDNF may have some effect on their response to stress.

Previously, we reported that decreased SHATI expression reduced the *Litaf* mRNA level in pheochromocytoma-12 cells that had been transfected with the vector containing shati cDNA [12]. In the present data, the reduction in *Litaf* expression in *Shati*-knockout mice was evidence that SHATI plays a role in LITAF expression in vivo. LITAF induces the expression of pre-inflammatory cytokines such as TNF-α [10]. A high level of TNF-α has been associated with symptoms of anxiety in humans under conditions of psychological stress [7]. However, absence of SHATI in the knockout mice resulted in anxiety behavior, despite the reduction in LITAF expression and the induction of BDNF expression in the prefrontal cortex and hippocampus. On the other hand, *Shati*-knockout mice spent longer periods of time with rearing in the open field test and exploration of objects in the novel object recognition test. Induction of BDNF may affect these exploration behaviors.

In conclusion, *Shati*-knockout may affect behavior. These changes in behavior may depend on the alteration of expression of various factors, i.e., BDNF, GDNF and LITAF that are involved with mood disorders and psychiatric impairment.

Acknowledgments

Yoko Furukawa-Hibi is a research resident of the Japan Foundation for Aging and Health. This study was supported in part by a Comprehensive Research grant on Aging and Health from the Ministry of Health, Labor and Welfare of Japan; the Global Center of Excellence program 'Integrated Functional Molecular Medicine for Neuronal and Neoplastic Disorders' from the Ministry of Education, Culture, Sports, Science and Technology of Japan; a Grant-in-aid for Exploratory Research and Scientific Research from the JSPS (Kakenhi); a Smoking Research Foundation Grant for Biomedical Research; an Academic Frontier Project grant for Private Universities (2007–2011) from the Ministry of Education, Culture, Sports, Science and Technology (MEXT) of Japan; and Funding Program for Next Generation World-Leading Researchers (NEXT Program).

References

[1] H. Anisman, Z. Merali, M.O. Poulter, S. Hayley, Cytokines as a precipitant of depressive illness: animal and human studies, Current Pharmaceutical Design 11 (2005) 963–972.
[2] P.S. Ariyannur, J.R. Moffett, P. Manickam, N. Pattabiraman, P. Arun, A. Nitta, T. Nabeshima, C.N. Madhavarao, A.M. Namboodiri, Methamphetamine-induced neuronal protein NAT8L is the NAA biosynthetic enzyme: implications for specialized acetyl coenzyme A metabolism in the CNS, Brain Research 1335 (2010) 1–13.
[3] Y. Furukawa-Hibi, T. Alkam, A. Nitta, A. Matsuyama, H. Mizoguchi, K. Suzuki, S. Moussaoui, Q.S. Yu, N.H. Greig, T. Nagai, K. Yamada, Butyrylcholinesterase inhibitors ameliorate cognitive dysfunction induced by amyloid-β peptide in mice, Behavioural Brain Research 225 (2011) 222–229.
[4] M. Hiramatsu, M. Sasaki, T. Nabeshima, T. Kameyama, Effects of dynorphin A (1-13) on carbon monoxide-induced delayed amnesia in mice, Pharmacology Biochemistry and Behavior 56 (1997) 73–79.
[5] A.V. Kalueff, P. Tuohimaa, Mouse grooming microstructure is a reliable anxiety marker bidirectionally sensitive to GABAergic drugs, European Journal of Pharmacology 508 (2005) 147–153.
[6] R.G. Lister, The use of a plus-maze to measure anxiety in the mouse, Psychopharmacology 92 (1987) 180–185.
[7] M. Maes, C. Song, A. Lin, R. De Jongh, A. Van Gastel, G. Kenis, E. Bosmans, I. De Meester, I. Benoy, H. Neels, P. Demedts, A. Janca, S. Scharpe, R.S. Smith, The effects of psychological stress on humans: increased production of pro-inflammatory cytokines and a Th1-like response in stress-induced anxiety, Cytokine 10 (1998) 313–318.
[8] S.F. Maier, L.R. Watkins, Cytokines for psychologists: implications of bidirectional immune-to-brain communication for understanding behavior, mood, and cognition, Psychological Review 105 (1998) 83–107.
[9] H. Miyagawa, M. Hasegawa, T. Fukuta, M. Amano, K. Yamada, T. Nabeshima, Dissociation of impairment between spatial memory, and motor function and emotional behavior in aged rats, Behavioural Brain Research 91 (1998) 73–81.
[10] F. Myokai, S. Takashiba, R. Lebo, S. Amar, A novel lipopolysaccharide-induced transcription factor regulating tumor necrosis factor α gene expression: molecular cloning, sequencing, characterization, and chromosomal assignment, Proceedings of the National Academy of Sciences of the United States of America 96 (1999) 4518–4523.
[11] A. Nakajima, K. Yamada, T. Nagai, T. Uchiyama, Y. Miyamoto, T. Mamiya, J. He, A. Nitta, M. Mizuno, M.H. Tran, A. Seto, M. Yoshimura, K. Kitaichi, T. Hasegawa, K. Saito, Y. Yamada, M. Seishima, K. Sekikawa, H.C. Kim, T. Nabeshima, Role of tumor necrosis factor-α in methamphetamine-induced drug dependence and neurotoxicity, Journal of Neuroscience 24 (2004) 2212–2225.
[12] M. Niwa, A. Nitta, X. Cen, K. Kitaichi, N. Ozaki, K. Yamada, T. Nabeshima, A novel molecule 'shati' increases dopamine uptake via the induction of tumor necrosis factor-α in pheochromocytoma-12 cells, Journal of Neurochemistry 107 (2008) 1697–1708.
[13] M. Niwa, A. Nitta, H. Mizoguchi, Y. Ito, Y. Noda, T. Nagai, T. Nabeshima, A novel molecule "shati" is involved in methamphetamine-induced hyperlocomotion, sensitization, and conditioned place preference, Journal of Neuroscience 27 (2007) 7604–7615.
[14] H. Qiao, Y. Noda, H. Kamei, T. Nagai, H. Furukawa, H. Miura, Y. Kayukawa, T. Ohta, T. Nabeshima, Clozapine, but not haloperidol, reverses social behavior deficit in mice during withdrawal from chronic phencyclidine treatment, Neuroreport 12 (2001) 11–15.
[15] M. Sarter, G. Bodewitz, D.N. Stephens, Attenuation of scopolamine-induced impairment of spontaneous alteration behaviour by antagonist but not inverse agonist and agonist β-carbolines, Psychopharmacology 94 (1988) 491–495.
[16] X. Tang, M.J. Fenton, S. Amar, Identification and functional characterization of a novel binding site on TNF-α promoter, Proceedings of the National Academy of Sciences of the United States of America 100 (2003) 4096–4101.
[17] S. Uchida, K. Hara, A. Kobayashi, K. Otsuki, H. Yamagata, T. Hobara, T. Suzuki, N. Miyata, Y. Watanabe, Epigenetic status of GDNF in the ventral striatum determines susceptibility and adaptation to daily stressful events, Neuron 69 (2011) 359–372.

Experimental Eye Research 93 (2011) 873–879

Contents lists available at SciVerse ScienceDirect

Experimental Eye Research

journal homepage: www.elsevier.com/locate/yexer

Periocular injection of *in situ* hydrogels containing Leu–Ile, an inducer for neurotrophic factors, promotes retinal ganglion cell survival after optic nerve injury

Masayoshi Nakatani [a,*], Yuko Shinohara [a], Miki Takii [a], Hisato Mori [a], Nobuharu Asai [a], Shigeru Nishimura [a], Yoko Furukawa-Hibi [b], Yoshiaki Miyamoto [c], Atsumi Nitta [c]

[a] *Bioengineering Institute, Research & Development Division, Nidek Co., Ltd., 13-2 Hama-cho, Gamagori, Aichi 443-0036, Japan*
[b] *Department of Neuropsychopharmacology & Hospital Pharmacy, Nagoya University Graduate School of Medicine, Nagoya 466-8850, Japan*
[c] *Department of Pharmaceutical Therapy & Neuropharmacology, Faculty of Pharmaceutical Science, Graduate School of Medicine and Pharmaceutical Science, University of Toyama, Toyama 930-0194, Japan*

ARTICLE INFO

Article history:
Received 26 April 2011
Accepted in revised form
30 September 2011
Available online 8 October 2011

Keywords:
Leu–Ile
periocular injection
neurotrophic factor
optic nerve injury
retinal ganglion cell

ABSTRACT

Intraocular administration of neurotrophic factors has been shown to delay irreversible degeneration of retinal ganglion cells (RGCs). It would be beneficial for the treatment of optic nerve (ON) injury if such neurotrophic factors could be delivered in a less-invasive manner. The dipeptide leucine–isoleucine (Leu–Ile) appears to induce the production of neurotrophic factors, including brain-derived neurotrophic factor (BDNF) and glial cell line-derived neurotrophic factor (GDNF), in the brain. We therefore administered Leu–Ile via periocular depot injection in rats and investigated the dipeptide's ability to induce BDNF and GDNF in the retina and to delay RGC loss in an ON injury model. Poloxamer–alginate hydrogels containing Leu–Ile were injected into the subconjunctival space of intact or ON-injured rats. BDNF and GDNF levels in the retina were determined by an enzyme immunoassay. Survival of RGCs was assessed in retinal flatmounts. Activation of extracellular signal-regulated kinases (ERK) and cAMP response element binding protein (CREB) in the retina was examined by Western blotting. At 2 h after injection of fluorescein isothiocyanate-conjugated Leu–Ile, the fluorescence intensities in the retina were 4.3-fold higher than those in the saline control. Treatment with Leu–Ile significantly increased the retinal levels of BDNF at 6 h and GDNF at 6–72 h after injection. Treatment with Leu–Ile significantly increased RGC survival to 14 days after ON injury and enhanced the activation of ERK at 72 h and CREB at 48 h after injection in the ON-injured retina. These results suggest that periocular delivery of Leu–Ile induces BDNF and GDNF production in the retina, which may eventually enhance RGC survival after ON injury.

1. Introduction

Damage to the optic nerve (ON) results in retrograde degeneration of retinal ganglion cells (RGCs), which may lead to visual loss. Unfortunately, there is no established treatment modality to preserve the RGCs and axons in optic neuropathies such as glaucoma. One of the mechanisms proposed to explain this RGC loss is a reduction in the levels of neurotrophic factors that those neurons receive from the brain via retrograde axonal transport (Dahlmann-Noor et al., 2010; Weber et al., 2010). Among these factors, exogenous brain-derived growth factor (BDNF) and glial cell line-derived neurotrophic factor (GDNF) have been shown to delay RGC loss after axotomy and ON crush in cats and rodents (Koeberle and Ball, 1998; Parrilla-Reverter et al., 2009; Dahlmann-Noor et al., 2010). Moreover, combined treatment with BDNF and GDNF promotes better survival of RGCs than does either factor used individually (Yan et al., 1999; Koeberle and Ball, 2002). However, the task of adequately delivering these macromolecules to the retina is challenging due to limited access to the retina and blood–ocular barriers. Systemic administration might deliver these factors to the retina, but this also carries a higher risk of untoward side effects. Intravitreal administration is an effective means of delivering therapeutic levels of these factors quickly with minimal systemic side effects, but it is an invasive procedure with complications such as cataract formation, vitreous hemorrhage, and endophthalmitis. Moreover, any RGC survival promoting effect after direct injection of neurotrophic factors into the eye is transient. Although periocular injection is a clinically well-tolerated and less-invasive

* Corresponding author. Tel.: +81 533 66 3030; fax: +81 533 66 3185.
E-mail address: masayoshi_nakatani@nidek.co.jp (M. Nakatani).

0014-4835/$ – see front matter © 2011 Elsevier Ltd. All rights reserved.
doi:10.1016/j.exer.2011.09.024

method than the intravitreal approach, it would be difficult for macromolecules to reach the retina and exhibit their survival promoting effects if administered in this manner.

We have reported that leucine–isoleucine (Leu–Ile), a hydrophobic dipeptide, induces BDNF and GDNF synthesis both in the striatum and in cultured mesencephalic neurons (Nitta et al., 2004). Leu–Ile also protects the brain from damage caused by administration of 6-hydroxydopamine and methamphetamine (Nitta et al., 2004; Niwa et al., 2007). In addition, Leu–Ile is known to increase GDNF expression through the Akt/cAMP response element binding protein (CREB), which is activated by the heat shock protein 90/Akt signaling pathway (Cen et al., 2006). Leu–Ile may thus be an effective small molecule for treating optic neuropathies. It is necessary, however, to ensure safe and adequate delivery to the target tissues to enable this dipeptide to be used as a therapeutic agent.

Poloxamer 407, a copolymer of ethylene oxide and propylene oxide blocks, exhibits *in situ* gelling behavior owing to its thermoreversible properties. The formulation has led to prolonged release profiles for many drug applications (Dumortier et al., 2006) as well as to the reduction of peptide degradation in tissues (Wenzel et al., 2002). In ocular applications, Poloxamer 407 is well-tolerated in periocular injection (Vehanen et al., 2007).

In the present study, we attempted to induce BDNF and GDNF in the retina by periocular injection of Leu–Ile by using a poloxamer-based solution as the vehicle, and investigated their effects on degeneration of RGCs after ON crush injury in rats.

2. Materials and methods

2.1. Preparation of in situ hydrogel containing Leu–Ile

Poloxamer 407 and sodium alginate were obtained from Sigma–Aldrich Japan (Tokyo, Japan). Poloxamer was added to cold 0.2% sodium alginate under continuous stirring until a homogenous solution was obtained (Vehanen et al., 2007; Lin et al., 2004). The final concentration of poloxamer was 20%. The polymer solution was autoclaved at 121 °C for 15 min. Leu–Ile or fluorescein isothiocyanate (FITC) conjugated Leu–Ile (FITC–Leu–Ile), prepared by American Peptide Company, Inc. (Sunnyvale, CA, USA), was dissolved in the poloxamer–alginate solution. The solutions were adjusted to a pH in the range of 6.8–7.4 with NaOH.

2.2. Animals

Wistar rats (Japan SLC, Shizuoka, Japan) were used in accordance with the ARVO Statement for the Use of Animals in Ophthalmic and Vision Research in protocols approved and monitored by the Institutional Animal Care and Use Committee of Nidek Co., Ltd. The animals were housed in a 12-h light and 12-h dark cycle and given standard chow and water *ad libitum*.

2.3. Periocular injections in rats

Male Wistar rats (8 weeks old, 240–275 g body weight) were anesthetized with a combination of ketamine (80 mg/kg) and xylazine (7 mg/kg) by intraperitoneal injection. One of the following solutions was injected into the temporal subconjunctival space using a 25-gauge needle with a glass syringe: 40 μL of the poloxamer–alginate solution, 0.9% saline containing FITC–Leu–Ile (0.17 μmol), or the poloxamer solution containing 0.8, 8.0, or 80 mM Leu–Ile (0.03, 0.33, and 3.3 μmol, respectively). The concentrations of Leu–Ile were chosen based on a preliminary study in which intravitreal injection of 0.03 μmol Leu–Ile remarkably increased both BDNF and GDNF levels in the retina (15.7-fold and 6.3-fold increase compared with saline vehicle injection, respectively). Each eye received one injection. The solution was kept on an ice block before injection to ensure that it was in liquid form. The animals were euthanized at the indicated times after injection by cutting the abdominal aorta under diethyl ether anesthesia, and the eyes were enucleated.

2.4. Fluorescence measurements

The sclera, choroid/retinal pigment epithelium (RPE), and retina were isolated from the eyeball. The ONs (between the optic chiasm and the eyeball) were removed from the brain. Each tissue was homogenized on ice with 500 μL PBS (pH 7.4) using a homogenizer (HG30; Hitachi Koki, Tokyo, Japan) for the sclera and ON, and an ultrasonicator (Sonifier250; Branson Japan, Tokyo, Japan) for the choroid/RPE and retina. The homogenate was allowed to sit on ice for 2 h, and then centrifuged at 14,000 *g* for 5 min. Fluorescence intensities (excitation at 495 nm, emission at 525 nm) of the supernatants were determined directly using a microplate spectrofluorometer (SpectraMax M2e; Molecular Devices Japan, Tokyo, Japan). Measurements were calibrated by measuring the fluorescence of serial dilutions of FITC–Leu–Ile standards, with corrections made for tissue autofluorescence using the values for an untreated eye.

2.5. Enzyme immunoassay

Levels of BDNF and GDNF protein expression were determined by enzyme immunoassay (EIA) (Nitta et al., 2004). Homogenate buffer (0.1 M Tris–HCl, pH 7.4) containing 1 M NaCl, 2% bovine serum albumin, 2 mM EDTA, and 0.2% sodium nitride was added to the retinal tissue at a ratio of 1 g wet tissue to 19 mL of buffer, pulse-sonicated for 100 s, and centrifuged at 100,000 *g* for 30 min. The supernatant was collected and used for the EIA.

2.6. Optic nerve crush injury and periocular injection

The rats were anesthetized with intraperitoneal injection of sodium pentobarbital (45 mg/kg). An incision was made in the temporal conjunctiva of the right eye, and the lateral rectus muscle was detached under an operating microscope. The optic nerve was exposed and isolated. Care was taken to avoid damaging small vessels around the optic nerve. A vascular clip (40 g micro-vascular clip; Bear Medic, Ibaraki, Japan) was then applied to the optic nerve at a distance of 1–2 mm posterior to the globe for 10 s to cause a crush injury (Karim et al., 2009). To confirm that retinal vessels retained patency, the retina was examined under an operating microscope immediately after the insult. The dissected conjunctiva was pushed back in place, and the eyelid sutured at the temporal canthus. At 30 min after the ON crush, 40 μL of the poloxamer–alginate solution containing 8 or 80 mM Leu–Ile was injected into the nasal subconjunctival space. The nasal side was selected to minimize leakage of the formed gel depot from the incision site.

2.7. Quantification of retinal ganglion cell rescue

The survival of RGCs was quantified by FluoroGold (FG; Biotium, Hayward, CA, USA) retrograde labeling of retinal flatmounts. After the rats were anesthetized with a mixture of ketamine and xylazine, 4 μL of FG dissolved in distilled water to a concentration of 2% was injected into the superior colliculus bilaterally at the following coordinates: 6.0 mm posterior to the bregma, 1.5 mm lateral to the midline, and 4.0 mm under the skull. This FG-labeling was conducted 3 days before euthanizing the rats in order to avoid overcounting RGCs by mistaking dye-engulfing macrophages and

microglia for labeled RGCs (Maeda et al., 2004; Tsai et al., 2008). The eyes were harvested from euthanized animals and fixed with 4% paraformaldehyde for 2 h. The isolated whole retinas were flat-mounted vitreous side up on a microscope slide, and examined under a 400× epifluorescence microscope (E800; Nikon, Tokyo, Japan) equipped with a filter set (excitation filter: 350–400 nm, barrier filter: 515 nm). FG-labeled RGCs were counted on a fluorescent digital micrograph in a masked fashion. On the micrograph, the retina was divided into twelve standard areas, with three areas (0.336 mm^2 in total) in each quadrant at 1, 2, and 3 mm from the optic nerve head. The density of labeled RGCs (cells/mm^2) was calculated for each retina from the average of 12 counts.

2.8. Western blotting

Western blot analysis of phosphorylated ERK and CREB was performed with modifications as described by Alkam et al. (2010). Briefly, the retinal tissues were homogenized in ice-cold extraction buffer (20 mM Trizma hydrochloride buffer [pH 7.6] containing 150 mM sodium chloride, 2 mM EDTA-2Na, 50 mM sodium fluoride, 10 mM sodium vanadate, 1% Nonidet P-40, 1% sodium deoxycholate, 0.1% sodium dodecyl sulfate [SDS], 1 mg/mL pepstatin, 1 mg/mL aprotinin, and 1 mg/mL leupeptin). Equal amounts of protein, 20 μg/lane, were resolved by 10% SDS–polyacrylamide gel electrophoresis, and then transferred to a polyvinylidene difluoride membrane (Millipore, Billerica, MA, USA). Membranes were incubated in 3% bovine serum albumin in phosphate-buffered saline containing 0.05% (v/v) Tween 20 for 2 h at room temperature. They were then independently incubated at 4 °C overnight with anti-ERK(1/2) phospho-threonine202/tyrosine204(pERK) rabbit antibody (Cell Signaling Technology, Beverley, MA, USA), anti-ERK(1/2) rabbit antibody (Cell Signaling Technology), anti-phospho-CREB rabbit antibody (Cell Signaling Technology), or anti-CREB rabbit antibody (Cell Signaling Technology). Next, the labeled proteins were allowed to react with horseradish peroxidase-conjugated anti-rabbit IgG (Amersham Biosciences, Piscataway, NJ, USA), and then readied for visualization by chemiluminescence (Western blotting detection reagents, Amersham Biosciences) according to the manufacturer's instructions. Quantification was performed using the image analysis software ImageQuant TL (GE Healthcare UK Ltd, Amersham, England).

2.9. Statistical analysis

All data are expressed as mean ± SEM. Statistical differences between two groups were determined with Student's *t* test. Statistical differences among three or more groups were determined with Dunnett's multiple comparison test. $P < 0.05$ was regarded as statistically significant.

3. Results

3.1. Leu–Ile amounts in tissue extractions

To estimate permeability of Leu–Ile into the posterior segments, poloxamer–alginate or saline containing FITC–Leu–Ile (0.17 μmol) was injected subconjunctivally in rat eyes. The poloxamer–alginate solution immediately formed a gel at the injection site. Table 1 shows the amount of FITC–Leu–Ile in extracts of sclera, choroid/RPE, retina, and optic nerve. In both the saline and poloxamer–alginate groups, the values were highest in the sclera and gradiently decreased toward the choroid/RPE, retina, and optic nerve at 2 h after injection. Compared with the saline group, the values of the poloxamer–alginate group were 14.4-fold, 15.0-fold, 4.3-fold, and 15.8-fold higher in the sclera, choroid/RPE, retina, and optic nerve, respectively.

Table 1
Amount of FITC–Leu–Ile in the posterior tissues of the eye after periocular injection in rats.

Time after injection	Tissue	FITC–Leu–Ile (pmol/tissue)	
		Saline	Poloxamer–alginate
2 h	Sclera	110.56 ± 17.70	1591.55 ± 120.29*
	Choroid/RPE	10.55 ± 1.98	158.27 ± 37.66*
	Retina	9.67 ± 2.65	41.53 ± 3.39*
	Optic nerve	0.70 ± 0.24	11.05 ± 3.89*
6 h	Sclera	10.16 ± 1.46	8.85 ± 1.06
	Choroid/RPE	0.62 ± 0.18	0.76 ± 0.19
	Retina	0.72 ± 0.11	0.91 ± 0.13
	Optic nerve	0.58 ± 0.09	1.20 ± 0.30

Data represented as mean ± SEM ($n = 4$–6 per group). FITC–Leu–Ile was injected into the subconjunctival space of intact rats. FITC–Leu–Ile, fluorescein isothiocyanate-conjugated Leu–Ile; RPE, retinal pigment epithelium. *: $P < 0.01$ vs. saline group.

However, they had decreased to levels comparable with those of the saline control by 6 h after injection.

3.2. Effect of Leu–Ile to induce production of BDNF and GDNF in retina

The time-course of BDNF and GDNF levels in the retina was examined by performing EIA at 6, 24, and 72 h after periocular injection of 3.3 μmol Leu–Ile into rat eyes. BDNF levels at 6 h were higher than those in the vehicle (hydrogel)-treated rats (Fig. 1A). GDNF levels increased 6–72 h after Leu–Ile treatment (Fig. 1B). Dose-response at 6 h revealed that 0.03 and 0.33 μmol Leu–Ile injection increased GDNF levels, while 3.3 μmol Leu–Ile injection increased both BDNF and GDNF levels compared with vehicle-only injection. Vehicle injection, however, also increased BDNF and GDNF levels compared with the saline control (Fig. 1C and D).

3.3. Effects of Leu–Ile to promote RGC survival in ON crush injury

RGC density in intact rat eyes was 2327 ± 36/mm^2 (cells/mm^2; mean ± SEM). By 14 days after ON crush, with saline or vehicle injection, RGC densities had decreased to 1105 ± 110/mm^2 and 1213 ± 88/mm^2, respectively. The eyes treated with 0.33 μmol Leu–Ile showed a greater RGC density (1752 ± 62/mm^2) compared with that of the saline/vehicle-treated group. Treatment with 3.3 μmol Leu–Ile also resulted in a higher RGC density (1563 ± 114/mm^2) compared with the saline/vehicle treatment (Fig. 2).

3.4. Effects of Leu–Ile on activation of ERK and CREB in ON-injured retina

To explore Leu–Ile-induced signal transduction in ON-injured retinas, activation of ERK and CREB were determined by Western blotting (Figs. 3 and 4). The activation of ERK and CREB was not altered in intact retinas or in ON-injured retinas with saline-treatment. Slight enhancement of ERK activation was observed in ON-injured retinas at 48 and 72 h after vehicle treatment (compared with normal). Treatment with 3.3 μmol Leu–Ile resulted in greater enhancement of ERK activation in ON-injured retinas at 48 h (compared with normal) and 72 h (compared with normal/saline/vehicle). Leu–Ile treatment also enhanced CREB activation in ON-injured retinas at 48 h (compared with normal/saline/vehicle).

4. Discussion

To estimate the penetration of Leu–Ile into the eye, we investigated changes in fluorescence in different posterior segments after periocular injection of poloxamer–alginate hydrogels containing

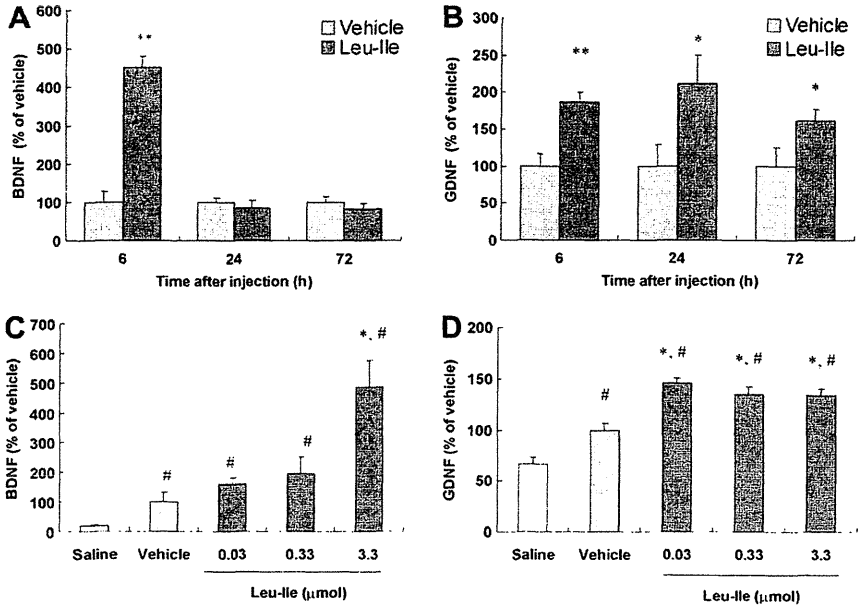

Fig. 1. Changes in BDNF (A, C) and GDNF (B, D) levels in rat retina after periocular injection of Leu–Ile. (A, B) Time-course of effects for 3.3 μmol Leu–Ile. Compared with the vehicle (hydrogel) group, both BDNF and GDNF levels were elevated at 6 h after treatment, but only GDNF levels remained elevated until 72 h. Data represented as mean ± SEM ($n = 7$–8 per group). **: $P < 0.01$, *: $P < 0.05$ vs. vehicle group. (C, D) Dose-response of Leu–Ile effects 6 h after treatment. BDNF levels were elevated with 3.3 μmol Leu–Ile, whereas GDNF levels were elevated with 0.03, 0.33, and 3.3 μmol Leu–Ile compared with the saline/vehicle group. Data represented as mean ± SEM ($n = 6$ per group). *: $P < 0.01$ vs. vehicle group; #: $P < 0.01$ vs. saline group.

FITC–Leu–Ile. We observed that the hydrogels remained on the sclera and enhanced Leu–Ile's permeability into the retina, which was the target tissue in this study, at 2 h after injection. By 6 h after injection, however, the hydrogels had become invisible on the sclera, and fluorescence in the tissues returned to levels comparable to those of the saline control (Table 1). Vehanen et al. (2007) have reported that periocular injection of 20% poloxamer solution facilitates absorption of small molecules (376 Da) into rat eye more

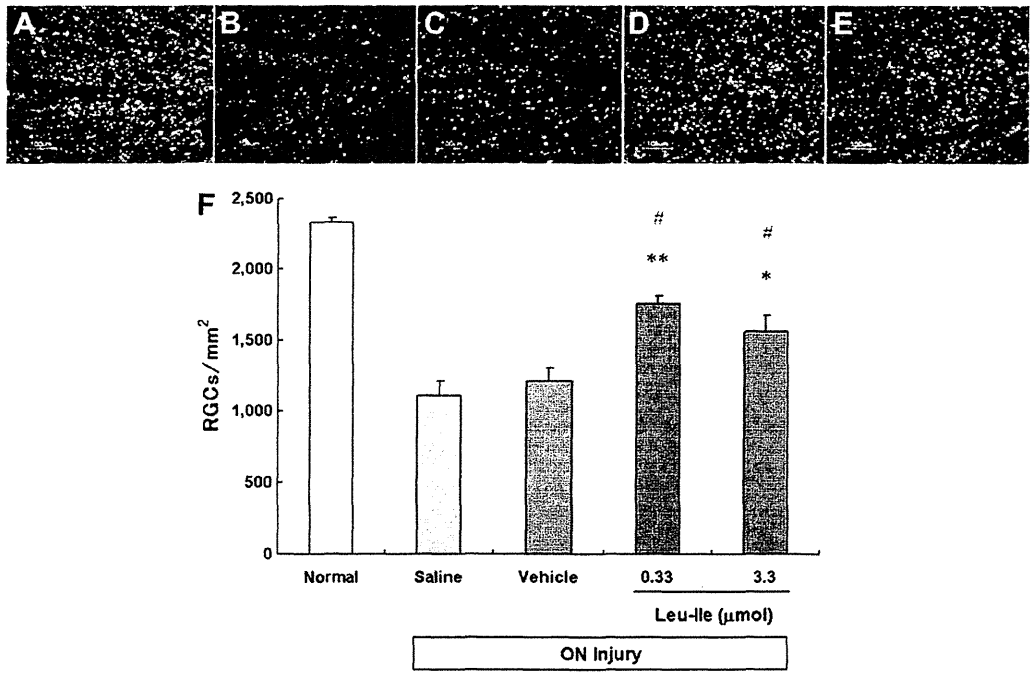

Fig. 2. Micrographs of flat-mounted retinas with retrograde labeling by FluoroGold and a graph showing RGC-rescue effects of periocular injection of Leu–Ile after optic nerve (ON) injury in rats. (A–E) Representative flat-mounted preparations of central areas of retinas. (A) Normal; (B) saline-treated with ON injury; (C) vehicle-treated with ON injury; (D) 0.33 μmol Leu–Ile-treated with ON injury; (E) 3.3 μmol Leu–Ile-treated with ON injury; (F) Density (in cells per square millimeter) of FluoroGold-labeled RGCs at 14 days after ON injury. Retinas treated with 0.33 and 3.3 μmol Leu–Ile showed higher RGC densities compared with saline/vehicle groups. Data represented as mean ± SEM ($n = 9$–10 per group). **: $P < 0.01$, *: $P < 0.05$ vs. vehicle group; #: $P < 0.01$ vs. saline group.

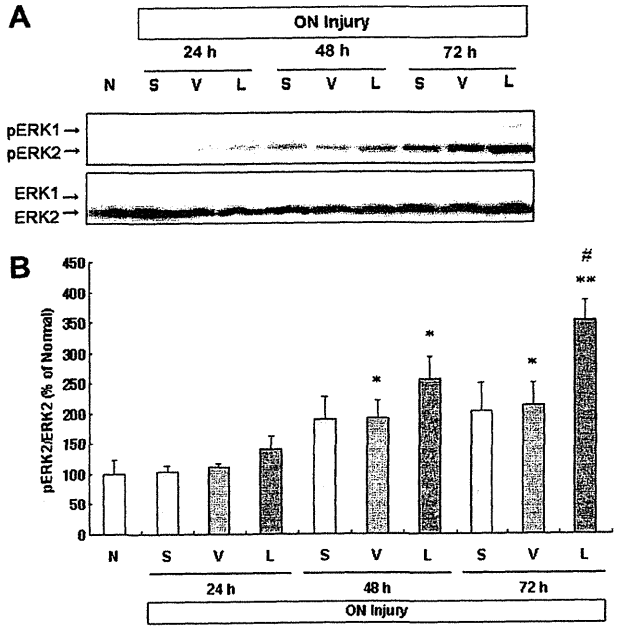

Fig. 3. Western blot analysis of pERK in rat retinas with optic nerve (ON) injury after periocular injection of Leu–Ile. (A) ERK phosphorylation was elevated in ON-injured retinas at 72 h after 3.3 μmol Leu–Ile treatment compared with saline/vehicle groups. N, Normal; S, Saline; V, Vehicle; L, Leu–Ile. (B) Densitometric analysis of ERK. The phosphorylation status of ERK2 is shown as the ratio of phosphorylated proteins to unphosphorylated proteins. Data represented as mean ± SEM ($n = 4$ per group). **: $P < 0.01$, *: $P < 0.05$ vs. normal; #: $P < 0.05$ vs. saline/vehicle groups.

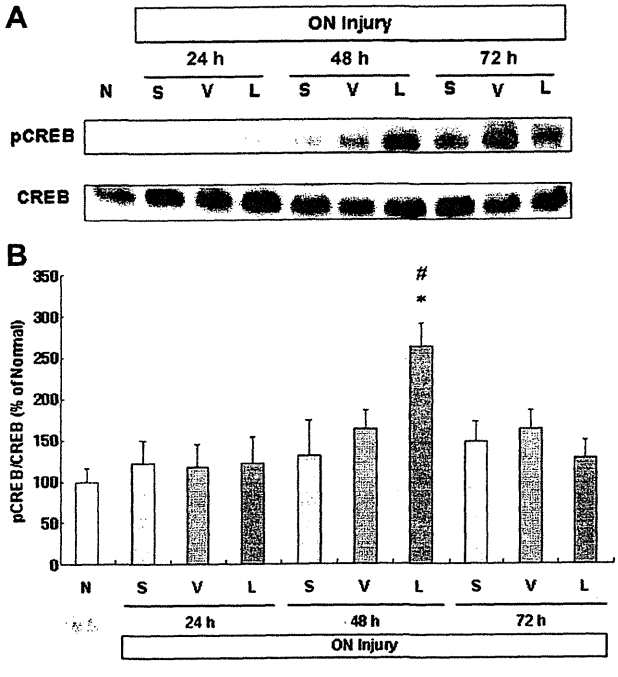

Fig. 4. Western blot analysis of pCREB in rat retinas with optic nerve (ON) injury after periocular injection of Leu–Ile. (A) CREB phosphorylation was elevated in ON-injured retinas at 48 h after 3.3 μmol Leu–Ile treatment compared with saline/vehicle groups. (B) Densitometric analysis of CREB. The phosphorylation status of CREB is shown as the ratio of phosphorylated proteins to unphosphorylated proteins. Data represented as mean ± SEM ($n = 4$ per group). *: $P < 0.01$ vs. normal; #: $P < 0.05$ vs. saline/vehicle groups.

effectively than larger molecules (4–40 kDa). However, the molecules' release from the poloxamer and absorption into the vitreous body only lasted for approximately 3 h. This relatively short-term interaction was also seen in our study. We used FITC–Leu–Ile because native Leu–Ile is a living component and is difficult to quantify in tissues. One possible limitation in our study is that our results may not precisely reflect the permeability of Leu–Ile into the eye because the molecular size of FITC–Leu–Ile is three times that of native Leu–Ile (244 Da). We confirmed in an *in vitro* experiment, however, that 80% of Leu–Ile is released into PBS from hydrogels containing 40 mM Leu–Ile within 8 h (data not shown). Our *in vivo* data are qualitatively similar to the quick-release profile found *in vitro*. Rieke et al. (2010) have reported that good correlation was obtained between their *in vitro* and *in vivo* release experiments when fluorescently-labeled protein was injected subconjunctivally using thermosetting hydrogel. We may therefore conjecture that the use of poloxamer–alginate as the vehicle improves bioavailability of Leu–Ile in a relatively short period of time. What would be more desirable, however, is more prolonged and controlled delivery.

Treatment with 3.3 μmol Leu–Ile increased BDNF and GDNF levels in the retina as early as at 6 h (Fig. 1). These results suggest that Leu–Ile can rapidly penetrate the blood–retinal barrier and reach target tissues at bioactive levels with this approach. Increased GDNF levels lasted for at least 3 days after the treatment, but increased levels of BDNF were not sustained. In addition, only GDNF levels increased with 0.03 μmol Leu–Ile, which was the lowest dose tested. The response was not dose-dependent. Cen et al. (2006) have reported that Leu–Ile binds to heat shock cognate protein 70 (Hsc70) and modulation of Hsc70 by this dipeptide triggers the transmission of neurotrophic signals, resulting in upregulation of GDNF expression. In rat retina, Hsc70 is strongly expressed in all layers, except the outer segments (Dean et al., 1999). Similarly, binding of Leu–Ile to Hsc70 seems to affect the increase of GDNF in retina. GDNF induction by Leu–Ile likely involves combinatorial interactions with multiple transcription factors. Moreover, Leu–Ile can also bind with other not yet defined proteins (unpublished data). Therefore, the lack of dose–response relationship may be attributed to the complicated cellular mechanisms underlying the GDNF-inducing effect of Leu–Ile. To investigate the effects of Leu–Ile on RGC survival, we tested two doses of Leu–Ile: 0.33 μmol, which stimulated only GDNF, and 3.3 μmol, which stimulated both BDNF and GDNF in intact rats. Treatment with Leu–Ile enhanced RGC survival, although there was no significant difference between the two dose groups (Fig. 2). These results may imply that the GDNF stimulated by Leu–Ile is principally involved in RGC-rescue.

Western blotting revealed that Leu–Ile had activated the ERK and CREB signaling pathways in ON-injured retinas by 48 and/or 72 h after treatment. These activations, however, were not observed at 24 h after treatment, in contrast to the increase in BDNF and GDNF levels that occurred as early as 6 h after treatment (Figs. 3 and 4). In a preliminary study, we observed that ON-crushing injury upregulated CREB in the retina at 6 h post injury, which then returned to the baseline level within 72 h (not significant, data not shown). Moreover, poloxamer–alginate by itself significantly induced BDNF and GDNF production, albeit to a relatively small extent (Fig. 1). These effects might hinder the specific effects of Leu–Ile in early phases. Poloxamer–alginate also significantly increased ERK activation 48 and 72 h after treatment (Fig. 3). The increases may be attributed to poloxamer 407, the main component of the hydrogel. Although the effects of poloxamer 407 (12,600 Da) on neural tissues are unknown, it has been reported that poloxamer 188 (8400 Da), another tri-block copolymer of ethylene oxide and propylene oxide, repairs cell membrane damage after traumatic brain injury and activates ERK in PC2 cells (a subline-derived from rat pheochromocytoma cell line PC12) (Serbest et al., 2006). It is possible that

poloxamer 407 or its degradation products act on the retinal cell membrane to increase BDNF and GDNF production and consequently activate ERK. Several reports have suggested that activation of ERK and CREB is necessary in the signaling needed to rescue RGCs in ON-axotomized (Choi et al., 2003) or injured retinas (Biermann et al., 2010). BDNF is capable of activating both the ERK pathway (Nakazawa et al., 2002) and CREB, which is induced by ERK (Fujino et al., 2009), in the retina. Although GDNF signaling in retinal protection is not fully understood, it has been shown to activate several ERK pathways in cultured retinal tissues (Hauck et al., 2006). The results of our Western blotting therefore support the hypothesis that Leu–Ile exerts an RGC survival promoting effect via the induction of BDNF and/or GDNF expression. Cen et al. (2006) have additionally reported that Leu–Ile rapidly stimulates both Akt and CREB phosphorylation, which in turn induce GDNF in cultured hippocampal neurons. Therefore, it may be possible that Leu–Ile delays RGC loss without the induction of neurotrophic factors. However, we have previously reported that Leu–Ile attenuated the methamphetamine-induced place preference of mice, while such attenuation by Leu–Ile was not observed in heterozygous knockout (GDNF(+/−)) mice (Niwa et al., 2007). Leu–Ile also inhibited the prolonged immobility time induced by the forced swimming test in mice, while such a reduction in immobility time was not observed in heterozygous knockout (BDNF(+/−)) mice (Furukawa-Hibi et al., 2011). These results suggest that the effects of Leu–Ile depend on BDNF or GDNF expression. This is one possibility that needs to be tested in ON-injured models in the future.

Sustained delivery of neurotrophic factors to the retina is an attractive approach for treating optic neuropathies. Intravitreal injection of biodegradable GDNF microspheres enabled prolonged delivery of GDNF in the retina and rescued RGCs in glaucoma and retinal ischemic models (Jiang et al., 2007; Kyhn et al., 2009). Intravitreal injection of viral vectors encoding neurotrophic factors or of stem cells also results in a prolonged effect on RGC survival in glaucoma and ON-injured models (Schmeer et al., 2002; Martin et al., 2003; Yu et al., 2006). In comparison with these studies, utilization of a hydrogel vehicle for periocular injection cannot offer a sustained delivery of Leu–Ile to the retina; therefore, it may not exert a prolonged effect on RGC survival. It does, however, appear to be a safer approach.

In conclusion, our results indicate that periocular injection of Leu–Ile using *in situ* hydrogels promotes BDNF and GDNF production in the retina and enhances survival of RGCs after ON injury. Leu–Ile may activate ERK and CREB signaling via the induction of these neurotrophic factors. Longer-term periocular delivery of Leu–Ile may be useful for the treatment of RGC degenerative diseases.

Acknowledgments

This project was financially supported by the Collaborative Development of Innovative Seeds program (Potentiality verification stage) of the Japan Science and Technology Agency.

References

Alkam, T., Nitta, A., Furukawa-Hibi, Y., Niwa, M., Mizoguchi, H., Yamada, K., Nabeshima, T., 2010. Oral supplementation with Leu–Ile, a hydrophobic dipeptide, prevents the impairment of memory induced by amyloid beta in mice via restraining the hyperphosphorylation of extracellular signal-regulated kinase. Behav. Brain Res. 210, 184–190.

Biermann, J., Grieshaber, P., Goebel, U., Martin, G., Thanos, S., Di Giovanni, S., Lagrèze, W.A., 2010. Valproic acid-mediated neuroprotection and regeneration in injured retinal ganglion cells. Invest. Ophthalmol. Vis. Sci. 51, 526–534.

Cen, X., Nitta, A., Ohya, S., Zhao, Y., Ozawa, N., Mouri, A., Ibi, D., Wang, L., Suzuki, M., Saito, K., Ito, Y., Kawagoe, T., Noda, Y., Ito, Y., Furukawa, S., Nabeshima, T., 2006. An analog of a dipeptide-like structure of FK506 increases glial cell line-derived neurotrophic factor expression through cAMP response element-binding protein activated by heat shock protein 90/Akt signaling pathway. J. Neurosci. 26, 3335–3344.

Choi, J.S., Kim, J.A., Joo, C.K., 2003. Activation of MAPK and CREB by GM1 induces survival of RGCs in the retina with axotomized nerve. Invest. Ophthalmol. Vis. Sci. 44, 1747–1752.

Dahlmann-Noor, A.H., Vijay, S., Limb, G.A., Khaw, P.T., 2010. Strategies for optic nerve rescue and regeneration in glaucoma and other optic neuropathies. Drug Discov. Today 15, 287–299.

Dean, D.O., Kent, C.R., Tytell, M., 1999. Constitutive and inducible heat shock protein 70 immunoreactivity in the normal rat eye. Invest. Ophthalmol. Vis. Sci. 40, 2952–2962.

Dumortier, G., Grossiord, J.L., Agnely, F., Chaumeil, J.C., 2006. A review of poloxamer 407 pharmaceutical and pharmacological characteristics. Pharm. Res. 23, 2709–2728.

Fujino, H., Kitaoka, Y., Hayashi, Y., Munemasa, Y., Takeda, H., Kumai, T., Kobayashi, S., Ueno, S., 2009. Axonal protection by brain-derived neurotrophic factor associated with CREB phosphorylation in tumor necrosis factor-alpha-induced optic nerve degeneration. Acta Neuropathol. 117, 75–84.

Furukawa-Hibi, Y., Nitta, A., Ikeda, T., Morishita, K., Liu, W., Ibi, D., Alkam, T., Nabeshima, T., Yamada, K., 2011. The hydrophobic dipeptide Leu–Ile inhibits immobility induced by repeated forced swimming via the induction of BDNF. Behav. Brain Res. 220, 271–280.

Hauck, S.M., Kinkl, N., Deeg, C.A., Swiatek-de Lange, M., Schöffmann, S., Ueffing, M., 2006. GDNF family ligands trigger indirect neuroprotective signaling in retinal glial cells. Mol. Cell Biol. 26, 2746–2757.

Jiang, C., Moore, M.J., Zhang, X., Klassen, H., Langer, R., Young, M., 2007. Intravitreal injections of GDNF-loaded biodegradable microspheres are neuroprotective in a rat model of glaucoma. Mol. Vis. 13, 1783–1792.

Karim, M.Z., Sawada, A., Mizuno, K., Kawakami, H., Ishida, K., Yamamoto, T., 2009. Neuroprotective effect of nipradilol [3,4-dihydro-8-(2-hydroxy-3-isopropylamino)-propoxy-3-nitroxy-2H-1-benzopyran] in a rat model of optic nerve degeneration. J. Glaucoma 18, 26–31.

Koeberle, P.D., Ball, A.K., 1998. Effects of GDNF on retinal ganglion cell survival following axotomy. Vision Res. 38, 1505–1515.

Koeberle, P.D., Ball, A.K., 2002. Neurturin enhances the survival of axotomized retinal ganglion cells in vivo: combined effects with glial cell line-derived neurotrophic factor and brain-derived neurotrophic factor. Neuroscience 110, 555–567.

Kyhn, M.V., Klassen, H., Johansson, U.E., Warfvinge, K., Lavik, E., Kiilgaard, J.F., Prause, J.U., Scherfig, E., Young, M., la Cour, M., 2009. Delayed administration of glial cell line-derived neurotrophic factor (GDNF) protects retinal ganglion cells in a pig model of acute retinal ischemia. Exp. Eye Res. 89, 1012–1020.

Lin, H.R., Sung, K.C., Vong, W.J., 2004. *In situ* gelling of alginate/pluronic solutions for ophthalmic delivery of pilocarpine. Biomacromolecules 5, 2358–2365.

Maeda, K., Sawada, A., Matsubara, M., Nakai, Y., Hara, A., Yamamoto, T., 2004. A novel neuroprotectant against retinal ganglion cell damage in a glaucoma model and an optic nerve crush model in the rat. Invest. Ophthalmol. Vis. Sci. 45, 851–856.

Martin, K.R., Quigley, H.A., Zack, D.J., Levkovitch-Verbin, H., Kielczewski, J., Valenta, D., Baumrind, L., Pease, M.E., Klein, R.L., Hauswirth, W.W., 2003. Gene therapy with brain-derived neurotrophic factor as a protection: retinal ganglion cells in a rat glaucoma model. Invest. Ophthalmol. Vis. Sci. 44, 4357–4365.

Nakazawa, T., Tamai, M., Mori, N., 2002. Brain-derived neurotrophic factor prevents axotomized retinal ganglion cell death through MAPK and PI3K signaling pathways. Invest. Ophthalmol. Vis. Sci. 43, 3319–3326.

Nitta, A., Nishioka, H., Fukumitsu, H., Furukawa, Y., Sugiura, H., Shen, L., Furukawa, S., 2004. Hydrophobic dipeptide Leu–Ile protects against neuronal death by inducing brain-derived neurotrophic factor and glial cell line-derived neurotrophic factor synthesis. J. Neurosci. Res. 78, 250–258.

Niwa, M., Nitta, A., Yamada, Y., Nakajima, A., Saito, K., Seishima, M., Shen, L., Noda, Y., Furukawa, S., Nabeshima, T., 2007. An inducer for glial cell line-derived neurotrophic factor and tumor necrosis factor-alpha protects against methamphetamine-induced rewarding effects and sensitization. Biol. Psychiatry 61, 890–901.

Parrilla-Reverter, G., Agudo, M., Sobrado-Calvo, P., Salinas-Navarro, M., Villegas-Pérez, M.P., Vidal-Sanz, M., 2009. Effects of different neurotrophic factors on the survival of retinal ganglion cells after a complete intraorbital nerve crush injury: a quantitative in vivo study. Exp. Eye Res. 15, 32–41.

Rieke, E.R., Amaral, J., Becerra, S.P., Lutz, R.J., 2010. Sustained subconjunctival protein delivery using a thermosetting gel delivery system. J. Ocul. Pharmacol. Ther. 26, 55–64.

Schmeer, C., Straten, G., Kügler, S., Gravel, C., Bähr, M., Isenmann, S., 2002. Dose-dependent rescue of axotomized rat retinal ganglion cells by adenovirus-mediated expression of glial cell-line derived neurotrophic factor in vivo. Eur. J. Neurosci. 15, 637–643.

Serbest, G., Horwitz, J., Jost, M., Barbee, K., 2006. Mechanisms of cell death and neuroprotection by poloxamer 188 after mechanical trauma. FASEB J. 20, 308–310.

Tsai, R.K., Chang, C.H., Wang, H.Z., 2008. Neuroprotective effects of recombinant human granulocyte colony-stimulating factor (G-CSF) in neurodegeneration after optic nerve crush in rats. Exp. Eye Res. 87, 242–250.

Vehanen, K., Hornof, M., Urtti, A., Uusitalo, H., 2007. Peribulbar poloxamer for ocular drug delivery. Acta Ophthalmol. 86, 91–96.

Weber, A.J., Viswanáthan, S., Ramanathan, C., Harman, C.D., 2010. Combined application of BDNF to the eye and brain enhances ganglion cell survival and function in the cat after optic nerve injury. Invest. Ophthalmol. Vis. Sci. 51, 327–334.
Wenzel, J.G., Balaji, K.S., Koushik, K., Navarre, C., Duran, S.H., Rahe, C.H., Kompella, U.B., 2002. Pluronic F127 gel formulations of deslorelin and GnRH reduce drug degradation and sustain drug release and effect in cattle. J. Control. Release 85, 51–59.
Yan, Q., Wang, J., Matheson, C.R., Urich, J.L., 1999. Glial cell line-derived neurotrophic factor (GDNF) promotes the survival of axotomized retinal ganglion cells in adult rats: comparison to and combination with brain-derived neurotrophic factor (BDNF). J. Neurobiol. 38, 382–390.
Yu, S., Tanabe, T., Dezawa, M., Ishikawa, H., Yoshimura, N., 2006. Effects of bone marrow stromal cell injection in an experimental glaucoma model. Biochem. Biophys. Res. Commun. 344, 1071–1079.

Behavioural Brain Research 210 (2010) 184–190

Contents lists available at ScienceDirect

Behavioural Brain Research

journal homepage: www.elsevier.com/locate/bbr

Research report

Oral supplementation with Leu-Ile, a hydrophobic dipeptide, prevents the impairment of memory induced by amyloid beta in mice via restraining the hyperphosphorylation of extracellular signal-regulated kinase

Tursun Alkam[a,b,c], Atsumi Nitta[a,e], Yoko Furukawa-Hibi[a], Minae Niwa[a,c], Hiroyuku Mizoguchi[a,d], Kiyofumi Yamada[a,e], Toshitaka Nabeshima[a,c,e,*]

[a] Department of Neuropsychopharmacology & Hospital Pharmacy, Nagoya University Graduate School of Medicine, Nagoya 466-8560, Japan
[b] Department of Basic Medicine, College of Traditional Uighur Medicine, Hotan 848-000, China
[c] Department of Chemical Pharmacology, Graduate School of Pharmaceutical Science, Meijo University, Nagoya 468-8503, Japan
[d] Futuristic Environmental Simulation Center, Research Institute of Environmental Medicine, Nagoya University, Nagoya 464-8601, Japan
[e] Japanese Drug Organization of Appropriate Use and Research, Nagoya 468-0069, Japan

ARTICLE INFO

Article history:
Received 15 November 2009
Received in revised form 6 February 2010
Accepted 12 February 2010
Available online 19 February 2010

Keywords:
Amyloid beta (25–35)
Extracellular signal-regulated kinase
Inducible nitric oxide synthase
Protein nitration
Novel object recognition memory

ABSTRACT

Restraining the toxic pathways of amyloid beta peptide (Aβ) by daily supplementation with dietary products has been shown effective in preventing cognitive decline. In this study, we examined the effects of the orally administered Leu-Ile, a hydrophobic dipeptide, on the neurotoxicity of $A\beta_{25-35}$ in mice. Chronic daily treatment with Leu-Ile prevented the $A\beta_{25-35}$-induced protein nitration and impairment of novel object recognition memory in mice. Protein nitration in the hippocampus induced by $A\beta_{25-35}$ was associated with the hyperphosphorylation of extracellular signal-regulated kinase (ERK) which was found responsible for the over-expression of inducible nitric oxide synthase. Sub-chronic treatment with Leu-Ile prevented the $A\beta_{25-35}$-induced hyperphosphorylation of ERK and protein nitration in the hippocampus. The results suggested that with the protective property against the neurotoxicity of $A\beta_{25-35}$, Leu-Ile could be considered as a candidate for the dietary supplementation in the prevention of Aβ-related impairment of recognition memory.

1. Introduction

Delaying or preventing the cognitive disorders in the elderly is a global imperative. The most studied cognitive disorder in modern history is Alzheimer's disease (AD), thanks to the assumption of amyloid beta peptide (Aβ) as the main player in its multifactor pathology. The recent advances in the understandings of the pathogenesis of AD propose the disruption of the neurotoxic pathways of Aβ as the main preventive approach to delay or control the progression of the disease [64,68]. However, the options for the preventive treatment are extremely limited due to the multifactor pathology that makes the management of AD a more complex process [16,31,38,43]. Further, the developments of new drugs take years before the general clinical application. Therefore, the oral supplements with the protective effects against Aβ should be considered for the immediate preventive treatment of AD.

The positive associations of the levels of cerebral Aβ and oxidative damage with the progression of the cognitive decline in the early stages of AD suggest an antioxidant- intervention strategy to delay the development of the disease [7,9,11,17,18,30,35,41,55,66]. In support, growing body of recent findings supports the use of dietary supplements with antioxidant capacity to retard the Aβ-associated decline of cognitive function in both animal and human [26,48,53,67,69].

The most abundant Aβ species in the brain of AD is $A\beta_{1-40}$. $A\beta_{1-40}$ can be truncated into a more toxic fragment $A\beta_{25-35}$ in the brain of AD [22]. $A\beta_{25-35}$ possesses the strongest oxidative capacity among all Aβ species [10,47,54]. Therefore, many recent studies applied $A\beta_{25-35}$ to investigate the usefulness of anti-oxidants in the protection against Aβ-induced impairment of memory in mice [12,32,61]. We have previously reported that restraining oxidative pathways of $A\beta_{25-35}$ that enhances nitration of protein (an indicator of oxidative damage) could prevent the impairments of memory in mice [3,4]. We have also reported that Leu-Ile, a hydrophobic dipeptide, protects against a neuronal damage induced by a strong oxidative reagent, 6-hydroxydopamine (6-OHDA) [39]. Therefore,

* Corresponding author at: Department of Chemical Pharmacology, Graduate School of Pharmaceutical Science, Meijo University, Nagoya 468-8503, Japan.
Tel.: +81 52 835 2735; fax: +81 52 839 2735.
E-mail addresses: tnabeshi@med.nagoya-u.ac.jp, tnabeshi@ccmfs.meijo-u.ac.jp (T. Nabeshima).

0166-4328/$ – see front matter © 2010 Elsevier B.V. All rights reserved.
doi:10.1016/j.bbr.2010.02.028

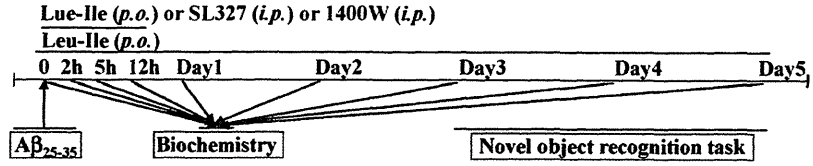

Fig. 1. Experimental schedule.

in this study, we have examined whether the oral supplementation with Leu-Ile could protect against $A\beta_{25-35}$-induced impairment of memory in mice. The results indicated that the oral treatment with Leu-Ile could prevent the enhanced nitration of protein in the hippocampus and the resultant impairment of novel object recognition memory in mice via restraining the hyperphosphorylation of extracellular signal-regulated kinase (ERK) induced by $A\beta_{25-35}$.

2. Materials and methods

2.1. Animals

Male, 5 weeks old ICR mice (Nihon SLC Co., Shizuoka, Japan), were used. The animals were housed in a controlled environment (23 ± 1 °C, 50 ± 5% humidity) and allowed food and water ad lib. The room lights were kept on between 8:00 a.m. and 8:00 p.m. All experiments were performed in accordance with the Guidelines for Animal Experiments of Nagoya University Graduate School of Medicine. The procedures involving animals and their care conformed to the Guidelines for Proper Conduct of Animal Experiments (Science Council of Japan, 2006).

2.2. Treatment and experimental design

$A\beta_{25-35}$ (Bachem, Bubendorf, Switzerland) was dissolved in sterile double-distilled water at the concentration of 1 mg/ml and stored at −20 °C before use and incubated for aggregation at 37 °C for 4 days before the injection [32]. The double distilled water was also incubated at the same condition as control. Incubated $A\beta_{25-35}$ (3 μg/3 μl) or incubated distilled water (control) (3 μl) was i.c.v.-injected as described previously [4,32]. Briefly, a microsyringe with a 28-gauge stainless-steel needle 3.0 mm long was used for all experiments. Mice were anesthetized lightly with ether, and the needle was inserted unilaterally 1 mm to the right of the midline point equidistant from each eye, at an equal distance between the eyes and the ears and perpendicular to the plane of the skull. A single-shot of the same volume (3 μl) of peptide or vehicle was delivered gradually within 3 s. Mice exhibited normal behaviour within 1 min after injection. The administration site was confirmed in preliminary experiments. Neither insertion of the needle nor the volume of injection had a significant influence on survival, and behavioural responses or cognitive functions.

Leu-Ile (Kokusan Chemical Co., Ltd., Tokyo, Japan) was dissolved in saline and was administered by either intraperitoneally (*i.p.*) or perorally (*p.o.*) at different doses which were decided according to a pilot study (unpublished data). The selective ERK inhibitor, α-[amino[(4-aminophenyl)thio]methylene]-2-(trifluoromethyl)-benzeneacetonitrile (SL327) (Sigma), was dissolved in dimethyl sulfoxide (DMSO). The selective inhibitor of iNOS, 1400W dihydrochloride (Sigma), was dissolved in normal saline (0.9% NaCl). The drugs were given by intraperitoneal (*i.p.*)-injection at indicated doses in a volume of 20 μl/10 g body weight [42].

The schedule of administration of peptides and drugs as well as biochemical and behavioral investigations is shown in Fig. 1.

2.3. Real-time reverse transcription-polymerase chain reaction

Mice were decapitated at the indicated time-points after the *i.c.v.*-injection of $A\beta_{25-35}$. The hippocampi were removed on ice-cold glass plate and stored at −80 °C. The hippocampal tissue was homogenized and total RNA was extracted using an RNeasy total RNA isolation kit, following the supplier's protocol (Qiagen, Valencia, CA). cDNA was synthesized by using a Superscript™ reverse transcriptase kit (Invitrogen, Carlsbad, CA). The primer sequences were given below: for TNF-α (Gene Bank access: NM_023517), forward primer: 5′-CTTTCGGTTGCTCTTTGGTTGAG-3′; reverse primer: 5′-GCAGCTCTGTCTGTTGGATCAG-3′; TaqMan probe: TGCGACAGCACAAGTCACAGCCCC; for the brain-derived neurotrophic factor (BDNF) (Gene Bank access: BC034862), forward primer: 5′-GCAAACATGTCTATGAGGGTTCG-3′; reverse primer: 5′-ACTCGCTAATACTGTCACACACG-3′; TaqMan probe: ACTCCGACCCTGCCCGCCGT; for glial cell-derived neurotrophic factor (GDNF) (Gene Bank access: NM_010275), forward primer: 5′-GAAGAGAGAGGAATCGGCAGG-3′; reverse primer: 5′-TGGCCTCTGCGACCTTTC-3′; TaqMan probe: AGCTGCCAGCCCAGAGAATTCCAGAG; For all, the experimental amplification protocol consisted of a first round at 95 °C for 3 min and then 30 cycles of denaturation at 95 °C for 60 s, annealing at 60 °C for 60 s, and extension at 72 °C for 1 min, with a final extension reaction carried out at 72 °C for 10 min. PCR was carried out on Bio-Rad iCycler iQ™ real-time PCR detection system (Bio-Rad Laboratories, Hercules, CA). The signal was detected according to the manufacturer's instructions. The expression levels were calculated as described previously [5].

2.4. Western blotting

Animals were decapitated at the indicated time-points after the injection of $A\beta_{25-35}$. The hippocampi were removed on ice-cold glass plate and stored at −80 °C. The hippocampal tissues were homogenized as described previously [3]. Briefly, the hippocampal tissues were homogenized in ice-cold extraction buffer (150 μl of 20 mM trizma hydrochloride buffer (pH 7.6) containing 150 mM sodium chloride, 2 mM EDTA·2Na, 50 mM sodium fluoride, 1 mM sodium vanadate, 1% Nonidet P-40, 1% sodium deoxycholate, 0.1% sodium dodecyl sulfate (SDS), 1 mg/ml pepstatin, 1 mg/ml aprotinin, and 1 mg/ml leupeptin). Equal amounts of protein, 20 μg/lane, were resolved by a 10% SDS-polyacrylamide gel electrophoresis, and then transferred electrophoretically to a polyvinylidene difluoride membrane (Millipore, Billerica, MA). Membranes were incubated in 3% skim milk (for nitrotyrosine and iNOS) or 3% bovine serum albumin (for phospho-proteins) in phosphate-buffered saline containing 0.05% (v/v) Tween 20 for 2 h at room temperature. Then the membranes were independently incubated at 4 °C overnight with anti-nitrotyrosine mouse monoclonal 1A6 antibody (Millipore, Billerica, MA), anti-iNOS rabbit polyclonal antibody (Upstate Biotechnology, Lake Placid, NY), anti-ERK(1/2) phospho-threonine202/tyrosine204 (p-ERK) rabbit antibody (Cell Signaling Technologies, Beverley, MA), anti-ERK(1/2) rabbit antibody (Cell Signaling Technologies, Beverley, MA), phospho and total anti-Jun N-terminal kinase (JNK) rabbit antibody (Santa Cruz Biotechnology Inc., Santa Crutz, CA), phospho and total anti-p38 MAPK rabbit antibody (Santa Cruz Biotechnology Inc., Santa Crutz, CA), and anti-β-actin goat antibody (Santa Cruz Biotechnology Inc., Santa Crutz, CA) were used. After washes, membranes were incubated with horseradish peroxidase-labeled anti-mouse IgG or anti-rabbit IgG (Kirkegaard & Perry Laboratories, Baltimore, MD) or with donkey anti-goat IgG secondary antibody (Santa Cruz Biotechnology Inc., Santa Crutz, CA). Immunoreactive complexes on the membrane were detected using Western blotting detection reagents (Amersham Biosciences Inc., Piscataway, NJ) according to the manufacturer's instructions, and exposed to X-ray film. The intensity of each protein band on the film was analyzed with the Atto Densitograph 4.1 system (Atto, Tokyo, Japan), and was corrected with the corresponding β-actin level. The results were expressed as the percentage of that of the control.

2.5. Novel object recognition task

This task, based on the spontaneous tendency of rodents to explore a novel object more often than a familiar one [15], was performed during Day 3 to Day 5 after the *i.c.v.*-injection of $A\beta_{25-35}$ (Day 0) as described previously [4]. A plastic chamber (35 cm × 35 cm × 35 cm) was used in low light condition during the light phase of the light/dark cycle. The general procedure consisted of three different phases: a habituation phase, an acquisition phase, and a retention phase. On the 1st day (habituation phase), mice were individually subjected to a single familiarization session of 10 min, during which they were introduced in the empty arena, in order to become familiar with the apparatus. On the 2nd day (acquisition phase) animals were subjected to a single 10-min session, during which floor-fixed two objects (A and B) were placed in a symmetric position from the centre of the arena, 15 cm from each and 8 cm from the nearest wall. The two objects, made of the same wooden material with the similar color and smell, were different in shape but identical in size. Mice were allowed to explore the objects in the open field. A preference index for each mouse was expressed as a ratio of the amount of time spent exploring object A (TA × 100)/(TA+TB), where TA and TB are the time spent on exploring object A and object B, respectively. On the 3rd day (retention phase), mice were allowed to explore the open field in the presence of two objects: the familiar object A and a novel object C in different shape but in similar color and size (A and C). A recognition index, calculated for each mouse, was expressed as the ratio (TC × 100)/(TA+TC), where TA and TC are the time spent during retention phase on object A and object C, respectively. The time spent exploring the object (nose pointing toward the object at a distance ≤1 cm) was recorded by hand.

2.6. Statistical analyses

The results are expressed as the mean ± S.E. Statistical significance was determined with one-way ANOVA followed by the Bonferroni multiple comparisons test. $p < 0.05$ was taken as a significant level of difference.

3. Results

3.1. Leu-Ile prevented impairment of memory via blocking protein nitration induced by $A\beta_{25-35}$

Daily treatments with Leu-Ile was commenced immediately before the *i.c.v.*-injection of $A\beta_{25-35}$ (Day 0) and continued (once a day) until Day 5. During the Day 3–5, the novel object recognition task was performed. During the acquisition phase of the task, all groups explored the two different objects for a similar amount of time (Fig. 2A). No differences among groups were observed concerning overall object exploration when different doses of Leu-Ile were administered. During the retention phase, the $A\beta_{25-35}$-injected mice did not discriminate the novel and familiar objects, and displayed a significantly decreased exploration to the new object in comparison with the control mice. Leu-Ile enhanced the new object discrimination ability of $A\beta_{25-35}$-injected mice (Fig. 2B). We have previously reported that chronic treatment with Leu-Ile can boost the mRNA levels of the brain-derived neurotrophic factor (BDNF), the glial cell line-derived neurotrophic factor (GDNF), and tumor necrosis factor-alpha (TNF-α) in the striatum of mice treated with 6-OHDA or methamphetamine [39,40]. It was therefore assumed that the enhanced expression of these factors by Leu-Ile might contribute to the amelioration of the $A\beta_{25-35}$-induced impairment of memory. As shown (Fig. 2C–E), the daily oral treatment with Leu-Ile did not change the mRNA levels of GDNF, BDNF, and TNF-α in the hippocampus (Day 5) of mice that received $A\beta_{25-35}$ injection (Day 0). The acute treatment with Leu-Ile did not change the mRNA levels of these factors in the hippocampus (data not shown). Daily treatment with Leu-Ile prevented $A\beta_{25-35}$-induced extensive nitration of hippocampal protein (indicated as nitrotyrosine) that appeared in a single band (Day 5) (Fig. 2F). We have previously confirmed the singularity of the band and identified the nitrated protein as neurofilament-L whose nitration is well associated with the impairment of memory in mice [3]. The above results suggested that the protective effect of Leu-Ile on the impairment of memory in mice could be due to the prevention of nitration of protein induced by $A\beta_{25-35}$.

3.2. Leu-Ile prevented $A\beta_{25-35}$-induced hyperphosphorylation of ERK

The intensity of nitration of proteins could be indicated by the elevation of the activity and protein level of inducible nitric oxide synthase (iNOS) induced by Aβ [37,52,58]. Both the activity and expression of iNOS are up-regulated by the persistent hyper-

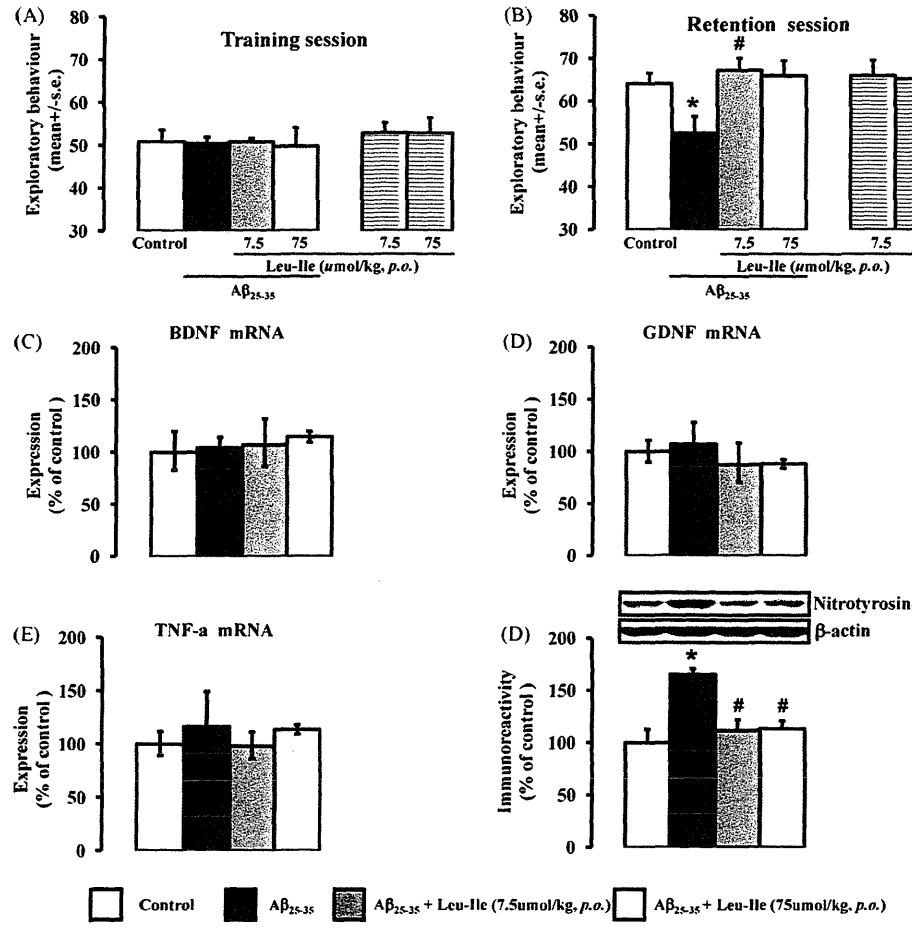

Fig. 2. Leu-Ile protects against memory impairment and hippocampal protein nitration induced by $A\beta_{25-35}$. Leu-Ile was administered immediately *p.o.* before the *i.c.v.*-injection of $A\beta_{25-35}$ (Day 0) and continued daily for next 5 consecutive days. (A and B) On Day 3–5 after the injection of $A\beta_{25-35}$, mice were subjected to the novel object recognition task. On training session (Day 4), neither $A\beta_{25-35}$ nor Leu-Ile affected the overall object exploration of mice. On retention session (Day 5), $A\beta_{25-35}$-injected mice displayed impairment of recognition memory. Treatment with Leu-Ile prevented the impairment of memory induced by $A\beta_{25-35}$. (C–E) Leu-Ile had no effect on the mRNA expression of GDNF, BDNF, and TNF-α in the hippocampus of $A\beta_{25-35}$-injected mice. (F) Increased nitration of hippocampal protein was found in $A\beta_{25-35}$-injected mice. Leu-Ile prevented the enhanced nitration of protein in the hippocampus induced by $A\beta_{25-35}$. Data were presented as the mean ± S.E., $n = 10$ for A and B; $n = 4$ for C–F; $^{*}p < 0.05$ vs. control. $^{\#}p < 0.05$ vs. $A\beta_{25-35}$. $A\beta_{25-35}$: Amyloid beta 25–35, GDNF: glia-drived neurotrophic factor, BDNF: brain-drived neurotrophic factor, TNF-α: tumor necrosis factor alpha.

phosphorylation of ERK, a member of mitogen activated protein kinase (MAPK) family [44,71]. We have previously reported the time dependent expression of iNOS mRNA by $A\beta_{25-35}$ [5]. We have therefore now examined the involvement of ERK and over-expression of iNOS protein in the neurotoxicity of $A\beta_{25-35}$. $A\beta_{25-35}$ enhanced the expression of iNOS protein in a time-dependent manner (Fig. 3A and B). $A\beta_{25-35}$ also persistently enhanced the phosphorylation of ERK at the time points that precedes the enhanced expression of iNOS (Fig. 3A and B). The phosphorylation of other members of MAPK family including c-Jun N-terminal kinase (JNK) and p38 were not affected by $A\beta_{25-35}$ (Fig. 3A and B). To examine the involvement of ERK in the induction of iNOS, we applied SL327, a selective inhibitor of the phosphorylation of ERK [42,63]. Since the inhibitory dose of SL327 (30 mg/kg, *i.p.*), which brings on the hypophosphorylation of ERK, did not prevent the impairment of memory induced by $A\beta_{25-35}$ and even impaired the memory in naïve mice (data not shown), we attempted to examine the sub-inhibitory dose of SL327 to restrain the $A\beta_{25-35}$-induced hyperphosphorylation of ERK without bringing on the hypophosphorylation. The lowest sub-inhibitory dose of SL327 (15 mg/kg, *i.p.*) on phosphorylation of ERK was identified in naïve mice (Fig. 3C). Treatment with SL327 at two doses (the inhibitory and sub-inhibitory), immediately before and 12 h after the *i.c.v.*-injection (at 0 h) of $A\beta_{25-35}$, almost identically prevented the enhanced expression of iNOS on Day 1 (at 24 h) (Fig. 3D). Selective inhibition of the activity of iNOS, with 1400W, prevented protein nitration on Day 1 induced by $A\beta_{25-35}$ (Fig. 3E). The results came with an agreement with the reports on the selective involvement of hyperphosphorylation of ERK in the regulation of iNOS [71] and in the oxidative toxicity of Aβ [1,13,24,33]. Treatment with SL327 (15 mg/kg, *i.p.*) immediately before and 12 h after the *i.c.v.*-injection of $A\beta_{25-35}$ prevented the hyperphosphorylation of ERK (on Day 1), protein nitration and impairment of memory (on Day 5) (Fig. 4A–D). The preventive effects of treatment with

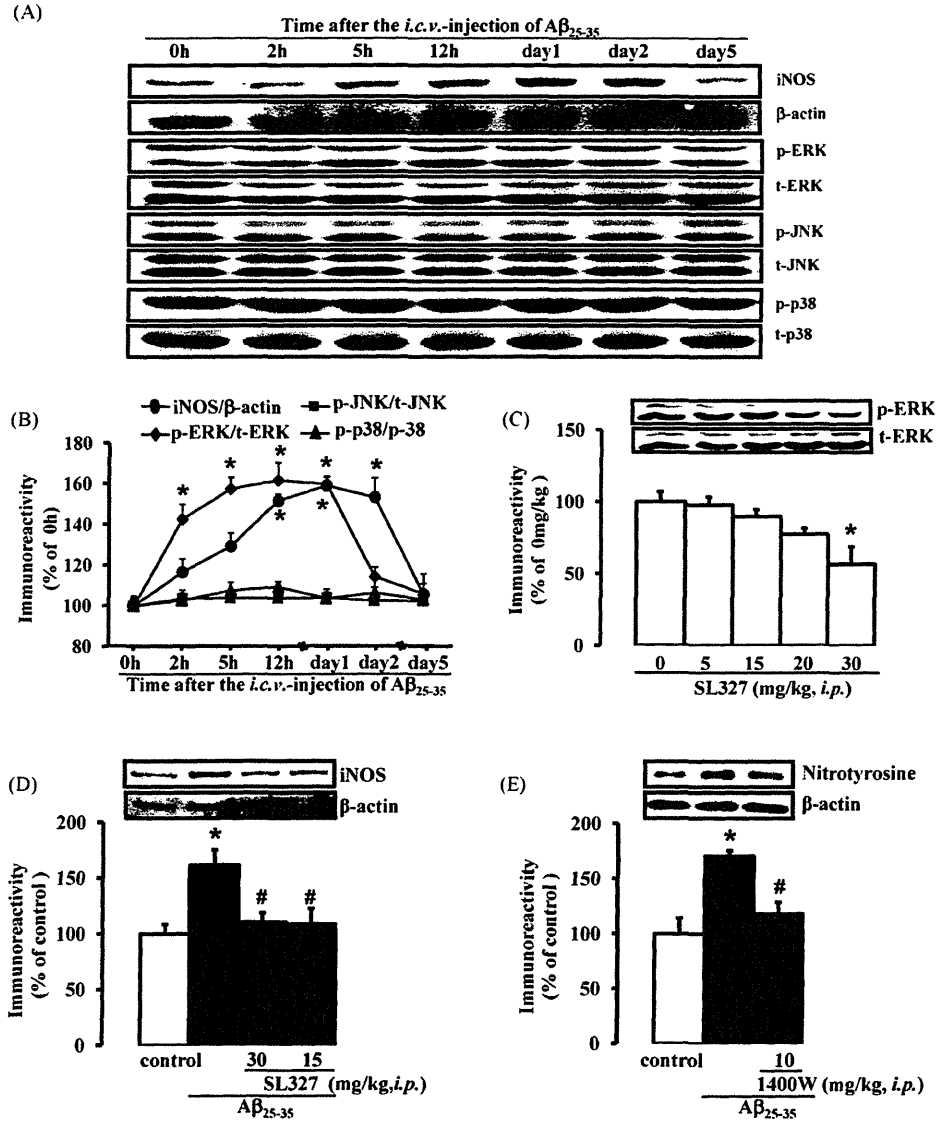

Fig. 3. Hyperphosphorylation of ERK is involved in the nitration of protein induced by $A\beta_{25-35}$. (A and B) At different time points after the *i.c.v.*-injection of $A\beta_{25-35}$ (0 h), the expression of iNOS and the phosphorylation levels of ERK, JNK, and p38 in the hippocampus were examined. Hyperphosphorylation of ERK precedes the enhanced expression of iNOS. The phosphorylation levels of JNK and p38 were not changed. (C and D) SL327, a selective inhibitor of ERK, was *i.p.*-injected at the inhibitory and sub-inhibitory doses immediately before and 12 h after the *i.c.v.*-injection of $A\beta_{25-35}$. Both doses prevented the enhanced expression of iNOS (at 24 h, or on Day 1) induced by $A\beta_{25-35}$. (E) Selective inhibition of iNOS by 1400W immediately before and 12 h after the *i.c.v.*-injection of $A\beta_{25-35}$ prevented the enhanced nitration of protein in the hippocampus. Data were presented as the mean ± S.E.; $n = 4$, $^{*}p < 0.05$ vs. control or 0 h or 0 mg/kg (SL327). $^{\#}p < 0.05$ vs. $A\beta_{25-35}$. $A\beta_{25-35}$: Amyloid beta 25–35.

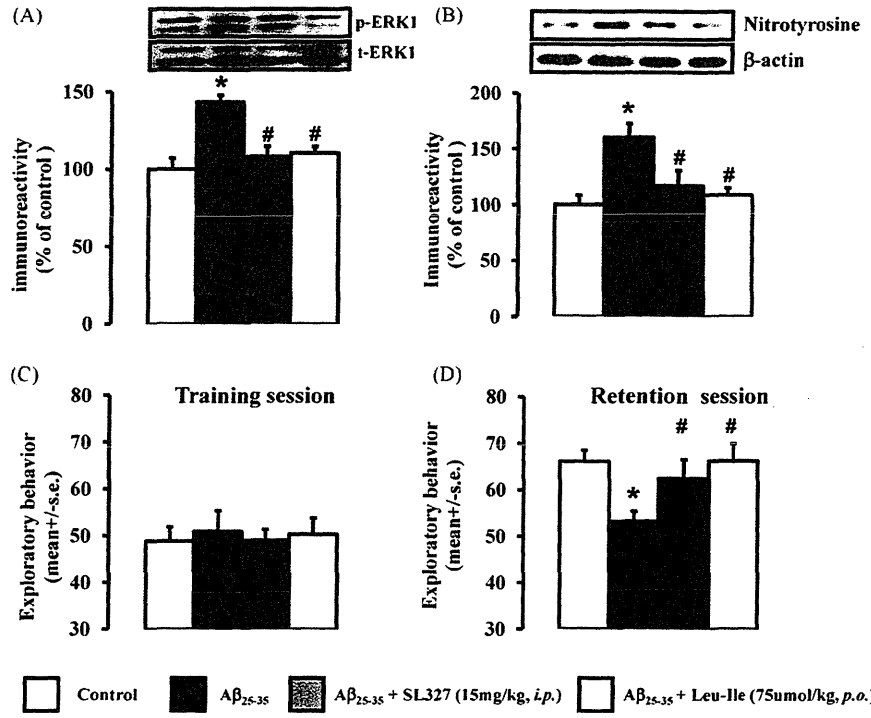

Fig. 4. Lue-Ile prevents the hyperphosphorylation of ERK induced by $A\beta_{25-35}$. (A and B) Sub-chronic treatment with SL327 or with Leu-Ile immediately before and 12 h after the *i.c.v.*-injection of $A\beta_{25-35}$ prevented the hyperphosphorylation of ERK (on Day 1), the enhanced nitration of protein (on Day 5) in the hippocampus and the impairment of memory (on Day 5) in mice. Data were presented as the mean ± S.E.; $n = 4$ for A and B, $n = 10$ for C and D. $^{*}p < 0.05$ vs. control. $^{\#}p < 0.05$ vs. $A\beta_{25-35}$. $A\beta_{25-35}$: Amyloid beta 25–35.

Leu-Ile immediately before and 12 h after the *i.c.v.*-injection of $A\beta_{25-35}$ were found to be same with those of SL327 (Fig. 4A–D) The results indicated that Leu-Ile protects the memory function in mice via restraining $A\beta_{25-35}$-induced hyperphosphorylation of ERK and resultant enhanced nitration of protein in the hippocampus.

4. Discussion

Providing a preventive alternative for the progressive cognitive decline in AD can improve the quality of lives of patients. In this study, we have provided one more alternative, a candidate of dietary supplement, for the prevention of Aβ-induced cognitive impairment. Oral administration of Leu-Ile protected against the nitration of proteins in the hippocampus and resultant impairment of memory in mice induced by $A\beta_{25-35}$ via regulating ERK.

In the early stage of AD pathology, the elevated levels of Aβ, phosphorylated ERK, and iNOS as well as peroxynitrite-mediated damage are associated with the progressive cognitive failure [28,45,46,55,59,62,65]. In their relationship, Aβ induces iNOS that mediates peroxynitrite damage via the hyperphosphorylation of ERK, while the selective inhibition of ERK or iNOS abolishes the neurotoxicity of Aβ [37,49].

Normally, ERK regulates a diverse array of functions through proper phosphorylation and dephosphorylation [60]. The transient enhancement in phosphorylation of ERK plays a critical role in the hippocampal synaptic plasticity as well as learning and memory [57]. The persistent increase in the phosphorylation of ERK is associated with the cell death [72] as well as the impairment of memory [14]. On the contrary, hypophosphorylation of ERK is also associated with the impairment of memory [70]. These diverse biological outcomes of ERK are decided by the physiological and pathological cellular environments as well as the cellular and subcellular localization of ERK [59]. The diversity and the accessibility of the potential substrates in the sub-cellular compartments also define the various cellular responses mediated by ERK [2].

The abnormal phosphorylation of ERK is persistently involved in the pathophysiology of AD. In the damaged areas of AD brain, the disease-stage-dependent abnormal phosphorylation of ERK is observed while the level of total ERK is not changed [29]. The hyperphosphorylation of ERK is found in the early stages of the pathological development of AD, while hypophosphorylation is found in the later stages [65]. The hyperphosphorylation of ERK mediates the neurotoxicity of Aβ [13,33,49] while the hypophosphorylation of ERK impairs the memory function [51,70]. At the early stage of exposure, Aβ generates hydrogen peroxide by reducing metal ions [21,56]. Aβ could also bind with catalase at a high affinity and inhibit the breakdown of hydrogen peroxide [34]. Scavenging of the hydrogen peroxide prevents the neurotoxicity of Aβ [6,8,27]. The hydrogen peroxide is global inducer of the hyperphosphorylation of ERK [25,36]. Further, the hyperphosphorylation of ERK is associated with the over-expression of iNOS [20,44,71] which elevates the level of nitric oxide in the cell and boosts the interaction of nitric oxide with superoxide to form prexoynitrite and the resultant nitration of protein [50]. The harmful outcome of the persistent hyperphosphorylation of ERK therefore could be due to the pathological environment that created by the elevated levels of hydrogen peroxide induced by Aβ [8,21,49].

The hyperphosphorylation of ERK mediates the cellular toxicity of 6-OHDA, a potent generator of hydrogen peroxide [19,23]. We have previously reported that Leu-Ile could protect against the cellular damage induced by 6-OHDA in mice [39]. In the present study, Leu-Ile prevented the hyperphosphorylation of ERK induced by $A\beta_{25-35}$. Whether or not Leu-Ile inhibits the production of hydrogen peroxide induced by $A\beta_{25-35}$ or scavenges hydrogen peroxide to prevent the hyperphosphorylation of ERK remains to be further studied.

In conclusion, Leu-Ile could be considered as the dietary supplement for the treatment of Aβ-related memory impairments.

Acknowledgments

This work was supported, in part, by the Japan-China Sasakawa Medical fellowship (to Tursun Alkam); by the Uehara Memorial Foundation fellowship for Foreign Researchers in Japan (to Tursun Alkam); by a Grant-in-Aid for the 21st Century Center of Excellence Program "Integrated Molecular Medicine for Neuronal and Neoplastic Disorders" and "Academic Frontier Project for Private Universities (2007–2011)" from the Ministry of Education, Culture, Sports, Science and Technology of Japan; by Comprehensive Research on Aging and Health from the Ministry of Health, Labor and Welfare of Japan; by the Japan-Canada Joint Health Research Program and Japan-France Joint Health Research Program (Joint Project from Japan Society for the Promotion of Science); and by an International Research Project Supported by the Meijo Asian Research Center.

References

[1] Abe K, Hisatomi R, Misawa M. Amyloid beta peptide specifically promotes phosphorylation and nuclear translocation of the extracellular signal-regulated kinase in cultured rat cortical astrocytes. J Pharmacol Sci 2003;93:272–8.
[2] Ajenjo N, Cañón E, Sánchez-Pérez I, Matallanas D, León J, Perona R, et al. Subcellular localization determines the protective effects of activated ERK2 against distinct apoptogenic stimuli in myeloid leukemia cells. J Biol Chem 2004;279:32813–23.
[3] Alkam T, Nitta A, Mizoguchi H, Itoh A, Murai R, Nagai T, et al. The extensive nitration of neurofilament light chain in the hippocampus is associated with the cognitive impairment induced by amyloid beta in mice. J Pharmacol Exp Ther 2008;327:137–47.
[4] Alkam T, Nitta A, Mizoguchi H, Itoh A, Nabeshima T. A natural scavenger of peroxynitrites, rosmarinic acid, protects against impairment of memory induced by Aβ25–35. Behav Brain Res 2007;180:139–45.
[5] Alkam T, Nitta A, Mizoguchi H, Saito K, Seshima M, Itoh A, et al. Restraining tumor necrosis factor-alpha by thalidomide prevents the amyloid beta-induced impairment of recognition memory in mice. Behav Brain Res 2008;189:100–6.
[6] Anderton B. Free radicals on the mind. Hydrogen peroxide mediates amyloid beta protein toxicity. Hum Exp Toxicol 1994;13:719.
[7] Bastianetto S, Quirion R. Natural antioxidants and neurodegenerative diseases. Front Biosci 2004;9:3447–52.
[8] Behl C, Davis JB, Lesley R, Schubert D. Hydrogen peroxide mediates amyloid beta protein toxicity. Cell 1994;77:817–27.
[9] Butterfield DA, Drake J, Pocernich C, Castegna A. Evidence of oxidative damage in Alzheimer's disease brain: central role for amyloid beta-peptide. Trends Mol Med 2001;7:548–54.
[10] Butterfield DA, Kanski J. Methionine residue 35 is critical for the oxidative stress and neurotoxic properties of Alzheimer's amyloid beta-peptide 1–42. Peptides 2002;23:1299–309.
[11] Butterfield DA, Reed TT, Perluigi M, De Marco C, Coccia R, Keller JN, et al. Elevated levels of 3-nitrotyrosine in brain from subjects with amnestic mild cognitive impairment: implications for the role of nitration in the progression of Alzheimer's disease. Brain Res 2007;1148:243–8.
[12] Choi J, Malakowsky CA, Talent JM, Conrad CC, Carroll CA, Weintraub ST, et al. Anti-apoptotic proteins are oxidized by Abeta25–35 in Alzheimer's fibroblasts. Biochim Biophys Acta 2003;1637:135–41.
[13] Chong YH, Shin YJ, Lee EO, Kayed R, Glabe CG, Tenner AJ. ERK1/2 activation mediates Abeta oligomer-induced neurotoxicity via caspase-3 activation and tau cleavage in rat organotypic hippocampal slice cultures. J Biol Chem 2006;281:20315–25.
[14] Enomoto T, Osugi T, Satoh H, McIntosh TK, Nabeshima T. Pre-Injury magnesium treatment prevents traumatic brain injury-induced hippocampal ERK activation, neuronal loss, and cognitive dysfunction in the radial-arm maze test. J Neurotrauma 2005;22:783–92.
[15] Ennaceur A, Delacour J. A new one-trial test for neurobiological studies of memory in rats. 1: Behavioral data. Behav Brain Res 1998;31:47–59.
[16] Greig NH, Giacobini E, Lahiri DK. Advances in Alzheimer therapy: development of innovative new strategies. Curr Alzheimer Res 2007;4:336–9.
[17] Grundman M, Grundman M, Delaney P. Antioxidant strategies for Alzheimer's disease. Proc Nutr Soc 2002;61:191–202.
[18] Guidi I, Galimberti D, Lonati S, Novembrino C, Bamonti F, Tiriticco M, et al. Oxidative imbalance in patients with mild cognitive impairment and Alzheimer's disease. Neurobiol Aging 2006;27:262–9.
[19] Heikkila R, Cohen G. Further studies on the generation of hydrogen peroxide by 6-hydroxydopamine. Potentiation by ascorbic acid. Mol Pharmacol 1972;8:241–8.
[20] Hua LL, Zhao ML, Cosenza M, Kim MO, Huang H, Tanowitz HB, et al. Role of mitogen-activated protein kinases in inducible nitric oxide synthase and TNFalpha expression in human fetal astrocytes. J Neuroimmunol 2002;126:180–9.
[21] Huang X, Atwood CS, Hartshorn MA, Multhaup G, Goldstein LE, Scarpa RC, et al. The A beta peptide of Alzheimer's disease directly produces hydrogen peroxide through metal ion reduction. Biochemistry 1999;38:7609–16.
[22] Kubo T, Nishimura S, Kumagae Y, Kaneko I. In vivo conversion of racemized beta-amyloid ([D-Ser 26]A beta 1–40) to truncated and toxic fragments ([D-Ser 26]A beta 25–35/40) and fragment presence in the brains of Alzheimer's patients. J Neurosci Res 2002;70:474–83.
[23] Kulich SM, Horbinski C, Patel M, Chu CT. 6-Hydroxydopamine induces mitochondrial ERK activation. Free Radic Biol Med 2007;43:372–83.
[24] Kuperstein F, Yavin E. ERK activation and nuclear translocation in amyloid-beta peptide- and iron-stressed neuronal cell cultures. Eur J Neurosci 2002;16:44–54.
[25] Lee WC, Choi CH, Cha SH, Oh HL, Kim YK. Role of ERK in hydrogen peroxide-induced cell death of human glioma cells. Neurochem Res 2005;30:263–70.
[26] Lim GP, Chu T, Yang F, Beech W, Frautschy SA, Cole GM. The curry spice curcumin reduces oxidative damage and amyloid pathology in an Alzheimer transgenic mouse. J Neurosci 2001;21:8370–7.
[27] Lovell MA, Xie C, Xiong S, Markesbery WR. Protection against amyloid beta peptide and iron/hydrogen peroxide toxicity by alpha lipoic acid. J Alzheimers Dis 2003;5:229–39.
[28] Luth HJ, Munch G, Arendt T. Aberrant expression of NOS isoforms in Alzheimer's disease is structurally related to nitrotyrosine formation. Brain Res 2002;953:135–43.
[29] Ma QL, Harris-White ME, Ubeda OJ, Simmons M, Beech W, Lim GP, et al. Evidence of Abeta- and transgene-dependent defects in ERK-CREB signaling in Alzheimer's models. J Neurochem 2007;103:1594–607.
[30] Marlatt MW, Lucassen PJ, Perry G, Smith MA, Zhu X. Alzheimer's disease: cerebrovascular dysfunction, oxidative stress, and advanced clinical therapies. J Alzheimers Dis 2008;15:199–210.
[31] Martínez A, Lahiri DK, Giacobini E, Greig NH. Advances in Alzheimer therapy: understanding pharmacological approaches to the disease. Curr Alzheimer Res 2009;6:83–5.
[32] Maurice T, Lockhart BP, Privat A. Amnesia induced in mice by centrally administered beta-amyloid peptides involves cholinergic dysfunction. Brain Res 1996;706:181–93.
[33] Medina MG, Ledesma MD, Domínguez JE, Medina M, Zafra D, Alameda F, et al. Tissue plasminogen activator mediates amyloid-induced neurotoxicity via Erk1/2 activation. EMBO J 2005;24:1706–16.
[34] Milton NG. Amyloid-beta binds catalase with high affinity and inhibits hydrogen peroxide breakdown. Biochem J 1999;344:293–6.
[35] Milton NG. Role of hydrogen peroxide in the aetiology of Alzheimer's disease: implications for treatment. Drugs Aging 2004;21:81–100.
[36] Milligan SA, Owens MW, Grisham MB. Differential regulation of extracellular signal-regulated kinase and nuclear factor-kappa B signal transduction pathways by hydrogen peroxide and tumor necrosis factor. Arch Biochem Biophys 1998;352:255–62.
[37] Nathan C, Calingasan N, Nezezon J, Ding A, Lucia MS, La Perle K, et al. Protection from Alzheimer's-like disease in the mouse by genetic ablation of inducible nitric oxide synthase. J Exp Med 2005;202:1163–9.
[38] Nelson PT, Braak H, Markesbery WR. Neuropathology and cognitive impairment in Alzheimer disease: a complex but coherent relationship. J Neuropathol Exp Neurol 2009;68:1–14.
[39] Nitta A, Nishioka H, Fukumitsu H, Furukawa Y, Sugiura H, Shen L, et al. Hydrophobic dipeptide Leu-Ile protects against neuronal death by inducing brain-derived neurotrophic factor and glial cell line-derived neurotrophic factor synthesis. J Neurosci Res 2004;78:250–8.
[40] Niwa M, Nitta A, Yamada Y, Nakajima A, Saito K, Seishima M, et al. An inducer for glial cell line-derived neurotrophic factor and tumor necrosis factor-alpha protects against methamphetamine-induced rewarding effects and sensitization. Biol Psychiatry 2007;61:890–901.
[41] Nunomura A, Perry G, Aliev G, Hirai K, Takeda A, Balraj EK, et al. Oxidative damage is the earliest event in Alzheimer disease. J Neuropathol Exp Neurol 2001;60:759–67.
[42] Ohno M, Frankland PW, Chen AP, Costa RM, Silva AJ. Inducible, pharmacogenetic approaches to the study of learning and memory. Nat Neurosci 2001;4:1238–43.
[43] Opar A. Mixed results for disease-modification strategies for Alzheimer's disease. Nat Rev Drug Discov 2008;7:717–8.
[44] Park JS, Woo MS, Kim SY, Kim WK, Kim HS. Repression of interferon-gamma-induced inducible nitric oxide synthase (iNOS) gene expression in microglia by sodium butyrate is mediated through specific inhibition of ERK signaling pathways. J Neuroimmunol 2005;168:56–64.
[45] Pei JJ, Braak H, An WL, Winblad B, Cowburn RF, Iqbal K, et al. Up-regulation of mitogen-activated protein kinases ERK1/2 and MEK1/2 is associated with the progression of neurofibrillary degeneration in Alzheimer's disease. Brain Res Mol Brain Res 2002;109:45–55.
[46] Perry G, Roder H, Nunomura A, Takeda A, Friedlich AL, Zhu X, et al. Activation of neuronal extracellular receptor kinase (ERK) in Alzheimer disease links oxidative stress to abnormal phosphorylation. Neuroreport 1999;10:2411–5.
[47] Pike CJ, Walencewicz-Wasserman AJ, Kosmoski J, Cribbs DH, Glabe CG, Cotman CW. Structure-activity analyses of beta-amyloid peptides: contributions of the beta 25–35 region to aggregation and neurotoxicity. J Neurochem 1995;64:253–65.

[48] Quinn JF, Bussiere JR, Hammond RS, Montine TJ, Henson E, Jones RE, et al. Chronic dietary alpha-lipoic acid reduces deficits in hippocampal memory of aged Tg2576 mice. Neurobiol Aging 2007;28:213–25.
[49] Rapoport M, Ferreira A. PD98059 prevents neurite degeneration induced by fibrillar beta-amyloid in mature hippocampal neurons. J Neurochem 2000;74:125–33.
[50] Reiter CD, Teng RJ, Beckman JS. Superoxide reacts with nitric oxide to nitrate tyrosine at physiological pH via peroxynitrite. J Biol Chem 2000;275:32460–6.
[51] Runyan JD, Dash PK. Intra-medial prefrontal administration of SCH-23390 attenuates ERK phosphorylation and long-term memory for trace fear conditioning in rats. Neurobiol Learn Mem 2004;82:65–70.
[52] Ryu JK, McLarnon JG. Minocycline or iNOS inhibition block 3-nitrotyrosine increases and blood-brain barrier leakiness in amyloid beta-peptide-injected rat hippocampus. Exp Neurol 2006;198:552–7.
[53] Sano M, Ernesto C, Thomas RG, Klauber MR, Schafer K, Grundman M, et al. A controlled trial of selegiline, alpha-tocopherol, or both as treatment for Alzheimer's disease. The Alzheimer's Disease Cooperative Study. N Engl J Med 1997;336:1216–22.
[54] Schubert D, Behl C, Lesley R, Brack A, Dargusch R, Sagara Y, et al. Amyloid peptides are toxic via a common oxidative mechanism. Proc Natl Acad Sci USA 1995;92:1989–93.
[55] Smith MA, Richey Harris PL, Sayre LM, Beckman JS, Perry G. Widespread peroxynitrite-mediated damage in Alzheimer's disease. J Neurosci 1997;17:2653–7.
[56] Tabner BJ, El-Agnaf OM, Turnbull S, German MJ, Paleologou KE, Hayashi Y, et al. Hydrogen peroxide is generated during the very early stages of aggregation of the amyloid peptides implicated in Alzheimer disease and familial British dementia. J Biol Chem 2005;280:35789–92.
[57] Thiels E, Klann E. Extracellular signal-regulated kinase, synaptic plasticity, and memory. Rev Neurosci 2001;12:327–45.
[58] Tran MH, Yamada K, Olariu A, Mizuno M, Ren XH, Nabeshima T. Amyloid beta-peptide induces nitric oxide production in rat hippocampus: association with cholinergic dysfunction and amelioration by inducible nitric oxide synthase inhibitors. FASEB J 2001;15:1407–9.
[59] Trojanowski JQ, Mawal-Dewan M, Schmidt ML, Martin J, Lee VM. Localization of the mitogen activated protein kinase ERK2 in Alzheimer's disease neurofibrillary tangles and senile plaque neurites. Brain Res 1993;618:333–7.
[60] Valjent E, Caboche J, Vanhoutte P. Mitogen-activated protein kinase/extracellular signal-regulated kinase induced gene regulation in brain: a molecular substrate for learning and memory? Mol Neurobiol 2001;23:83–99.
[61] Villard V, Espallergues J, Keller E, Alkam T, Nitta A, Yamada K, et al. Anti-amnesic and neuroprotective effects of the aminotetrahydrofuran derivative ANAVEX1-41 against amyloid beta(25–35)-induced toxicity in mice. Neuropsychopharmacology 2009;34:1552–66.
[62] Vodovotz Y, Lucia MS, Flanders KC, Chesler L, Xie QW, Smith TW, et al. Inducible nitric oxide synthase in tangle-bearing neurons of patients with Alzheimer's disease. J Exp Med 1996;184:1425–33.
[63] Wang X, Wang H, Xu L, Rozanski DJ, Sugawara T, Chan PH, et al. Significant neuroprotection against ischemic brain injury by inhibition of the MEK1 protein kinase in mice: exploration of potential mechanism associated with apoptosis. J Pharmacol Exp Ther 2003;304:172–8.
[64] Walsh DM, Selkoe DJ. Deciphering the molecular basis of memory failure in Alzheimer's disease. Neuron 2004;44:181–93.
[65] Webster B, Hansen L, Adame A, Crews L, Torrance M, Thal L, et al. Astroglial activation of extracellular-regulated kinase in early stages of Alzheimer disease. J Neuropathol Exp Neurol 2006;65:142–451.
[66] Yamada K, Nabeshima T. Animal models of Alzheimer's disease and evaluation of anti-dementia drugs. Pharmacol Ther 2000;88:93–113.
[67] Yamada K, Tanaka T, Han D, Senzaki K, Kameyama T, Nabeshima T. Protective effects of idebenone and alpha-tocopherol on beta-amyloid-(1–42)-induced learning and memory deficits in rats: implication of oxidative stress in beta-amyloid-induced neurotoxicity in vivo. Eur J Neurosci 1999;11:83–90.
[68] Yankner BA, Lu T. Amyloid beta-protein toxicity and the pathogenesis of Alzheimer disease. J Biol Chem 2009;284:4755–9.
[69] Zandi PP, Anthony JC, Khachaturian AS, Stone SV, Gustafson D, Tschanz JT, et al. Reduced risk of Alzheimer disease in users of antioxidant vitamin supplements: the Cache County Study. Arch Neurol 2004;61:82–8.
[70] Zhang HT, Zhao Y, Huang Y, Dorairaj NR, Chandler LJ, O'Donnell JM. Inhibition of the phosphodiesterase 4 (PDE4) enzyme reverses memory deficits produced by infusion of the MEK inhibitor U0126 into the CA1 subregion of the rat hippocampus. Neuropsychopharmacology 2004;29:1432–9.
[71] Zhang Y, Brovkovych V, Brovkovych S, Tan F, Lee BS, Sharma T, et al. Dynamic receptor-dependent activation of inducible nitric-oxide synthase by ERK-mediated phosphorylation of Ser745. J Biol Chem 2007;282:32453–61.
[72] Zhuang S, Schnellmann RG. A death-promoting role for extracellular signal-regulated kinase. J Pharmacol Exp Ther 2006;319:991–7.

Pathway-specific modulation of nucleus accumbens in reward and aversive behavior via selective transmitter receptors

Takatoshi Hikida[a,b,c,1], Satoshi Yawata[a], Takashi Yamaguchi[a,d], Teruko Danjo[a], Toshikuni Sasaoka[e], Yanyan Wang[f], and Shigetada Nakanishi[a,1]

[a]Department of Systems Biology, Osaka Bioscience Institute, Suita, Osaka 565-0874, Japan; [b]Department of Research and Drug Discovery, Medical Innovation Center, Kyoto University Graduate School of Medicine, Kyoto 606-8501, Japan; [c]Japan Science and Technology Agency, Precursory Research for Embryonic Science and Technology, Kawaguchi, Saitama 332-0012, Japan; [d]Department of Aging Science, Graduate School of Medicine, Osaka University, Suita, Osaka 565-0871, Japan; [e]Department of Laboratory Animal Science, Kitasato University School of Medicine, Sagamihara, Kanagawa 252-0374, Japan; and [f]Department of Pharmacology, Beckman Institute, University of Illinois, Urbana, IL 61801

Contributed by Shigetada Nakanishi, November 22, 2012 (sent for review October 22, 2012)

The basal ganglia–thalamocortical circuitry plays a central role in selecting actions that achieve reward-seeking outcomes and avoid aversive ones. Inputs of the nucleus accumbens (NAc) in this circuitry are transmitted through two parallel pathways: the striatonigral direct pathway and the striatopallidal indirect pathway. In the NAc, dopaminergic (DA) modulation of the direct and the indirect pathways is critical in reward-based and aversive learning and cocaine addiction. To explore how DA modulation regulates the associative learning behavior, we developed an asymmetric reversible neurotransmission-blocking technique in which transmission of each pathway was unilaterally blocked by transmission-blocking tetanus toxin and the transmission on the intact side was pharmacologically manipulated by local infusion of a receptor-specific agonist or antagonist. This approach revealed that the activation of D1 receptors and the inactivation of D2 receptors postsynaptically control reward learning/cocaine addiction and aversive learning in a direct pathway-specific and indirect pathway–specific manner, respectively. Furthermore, this study demonstrated that aversive learning is elicited by elaborate actions of NMDA receptors, adenosine A2a receptors, and endocannabinoid CB1 receptors, which serve as key neurotransmitter receptors in inducing long-term potentiation in the indirect pathway. Thus, reward and aversive learning is regulated by pathway-specific neural plasticity via selective transmitter receptors in the NAc circuit.

avoidance | decision-making | drug addiction | reward-based learning | synaptic plasticity

The basal ganglia circuitry plays a central role in integrating neural information from the cerebral cortex and thalamus to facilitate selection of actions that achieve reward-seeking outcomes and avoid aversive outcomes (1, 2). Dysfunction of the basal ganglia leads to devastating cognitive and psychiatric disorders in Parkinson disease, schizophrenia, and drug addiction (3–5). The projection neurons of the striatum and the nucleus accumbens (NAc), which is a ventral part of the striatum, are divided into two subpopulations (i.e., the striatonigral neurons in the direct pathway and the striatopallidal neurons in the indirect pathway). Inputs of these two parallel pathways converge at the substantia nigra pars reticulata (SNr) and control the dynamic balance of the basal ganglia–thalamocortical circuitry (6–8). In this circuit, dopamine (DA) from the ventral tegmental area (VTA) is essential for associative learning by dichotomously controlling glutamatergic synaptic plasticity in the direct and indirect pathways of the NAc via D1 and D2 receptors, respectively (9, 10). Furthermore, several key neurotransmitters including NMDA receptors, adenosine A2a receptors, and endocannabinoid CB1 receptors have been shown to be involved in DA-modulated synaptic plasticity in either or both pathways of the corticostriatal circuit (10–13). However, the regulatory mechanisms of these two parallel pathways in associative learning behaviors and, in particular, the synaptic mechanisms involved in aversive learning have still largely remained to be elucidated.

In a previous study, we developed a gene-manipulating technique termed reversible neurotransmission blocking (RNB) in which transmission of the direct or the indirect pathway is separately and reversibly blocked by pathway-specific expression of the transmission-blocking tetanus toxin in a doxycycline-regulated manner (14). Blockade of the direct pathway markedly attenuates both appetitive reward learning and cocaine sensitization. In contrast, when the indirect pathway is blocked, the ability to induce reward-based learning and cocaine sensitization is retained but aversive learning is impaired.

The function of the basal ganglia circuitry becomes defective only when both sides of the NAc circuit are simultaneously impaired in the brain hemispheres (15, 16). We thus extended the RNB technique to an asymmetric RNB (aRNB) technique. In this technique, one side of the NAc was blocked by the RNB technique and the other intact side was treated with an agonist or antagonist specific for a neurotransmitter receptor (17). This aRNB technique allowed us to examine what types of neurotransmitter receptors were responsible for learning in a pathway-specific and learning stage–dependent manner. Here, we report that the pathway-specific D1 receptor activation and D2 receptor inactivation distinctly control reward-based learning and aversive learning, respectively, and that a set of the neurotransmitter receptors that induce long-term potentiation (LTP) in the indirect pathway are indispensable for inducing aversive learning.

Results

Analytical Strategy for Assessing Pathway-Specific, DA Receptor–Dependent Behavior. In the RNB technique, bilateral transmission blockade of either the direct pathway (D-RNB mice) or the indirect pathway (I-RNB mice) was achieved by the pathway-specific expression of transmission-blocking tetanus toxin, which was driven by interaction of the tetracycline-repressive transcription factor (tTA) and the tetracycline-responsive element (TRE) (14). The specific expression of tTA was made by using the adeno-associated virus (AAV)-mediated expression system, in which the tTA expression in the direct and indirect pathways was driven by the substance P and the enkephalin promoters, respectively (14). In the aRNB technique (Fig. 1*A*), transmission in either the direct pathway (D-aRNB mice) or the indirect

Author contributions: T.H. and S.N. designed research; T.H., S.Y., T.Y., and T.D. performed research; T.S. and Y.W. contributed new reagents/analytic tools; T.H. analyzed data; and T.H. and S.N. wrote the paper.

The authors declare no conflict of interest.

[1]To whom correspondence may be addressed. E-mail: snakanis@obi.or.jp or hikida@tk.med.kyoto-u.ac.jp.

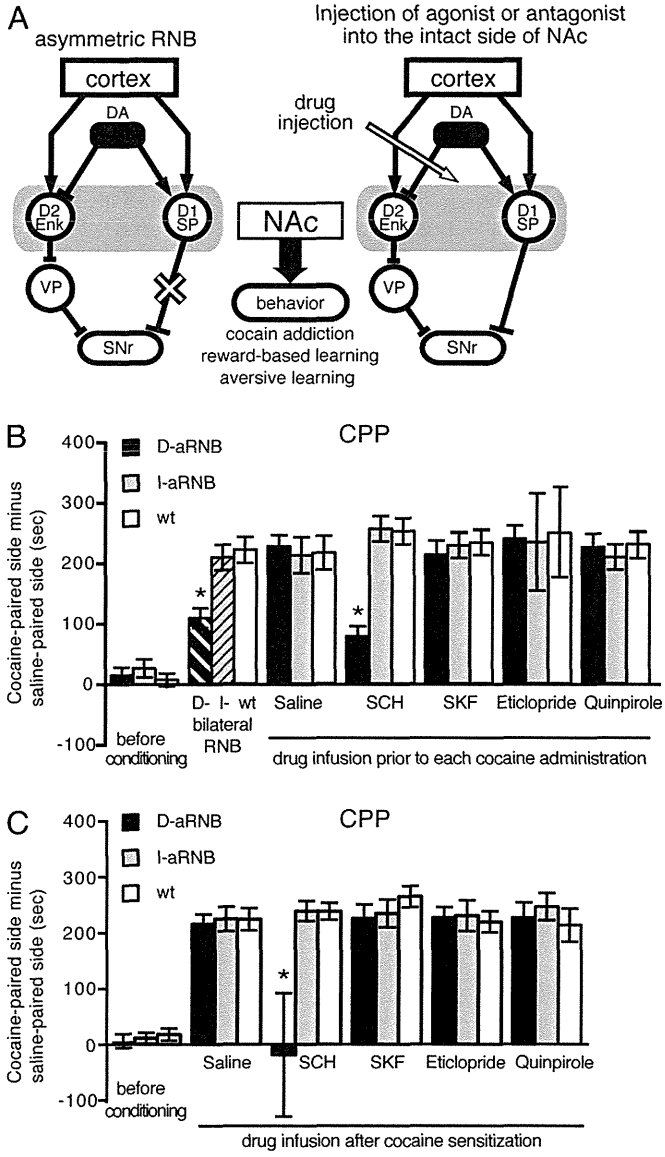

Fig. 1. Acquisition and expression of cocaine-induced CPP by D1 receptor activation in the direct pathway. (*A*) Schema of the asymmetric RNB technique combined with pharmacological analysis. One side of transmission of the direct or indirect pathway in the NAc was blocked by the RNB technique (as indicated by the ×), and the other intact side of the NAc was injected with saline or an agonist or antagonist specific for the targeted receptor. Arrowed and blocked lines note excitatory and inhibitory transmissions, respectively. D1, D1 receptors; D2, D2 receptors; Enk, enkephalin; SNr, substantia nigra pars reticulata; SP, substance P; VP, ventral pallidum. (*B*) Saline or the indicated DA agent was injected into the NAc 20 min before place conditioning of mice with administration of 10 mg/kg cocaine at one fixed chamber and saline at the other chamber. This conditioning was daily conducted for 3 d, and CPP was tested on day 4 without injection of the DA agent and cocaine administration (n = 5–6). (*C*) Mice were conditioned by administration of 10 mg/kg cocaine for 3 d. On day 4, saline or the indicated DA agent was injected; and 20 min later, CPP was measured without cocaine administration (n = 5–6). Columns and bars represent the mean ± SEM, respectively. D-RNB vs. I-RNB/WT or D-aRNB vs. I-aRNB/WT, $^*P < 0.05$.

pathway (I-aRNB mice) of the NAc was unilaterally blocked by the RNB technique. Then, 2–3 wk after the viral injection, a neurotransmitter agonist or antagonist was injected into the intact side of the NAc through an implanted cannula. Animal behavior was analyzed 20 min after drug infusion (Fig. 1*A*). After the behavioral analysis had been completed, the location of the implanted cannula was confirmed. A D1 agonist, SKF81297 (SKF), and a D1 antagonist, SCH23390 (SCH), were used to examine involvement of D1 receptors; whereas a full D2 agonist, quinpirole, a partial D2 agonist, aripiprazole, and a D2 antagonist, eticlopride, were used to examine engagement of D2 receptors.

Selective Role of D1 Receptor–Dependent Direct Pathway in Cocaine Addiction. Conditioned place preference (CPP) is associative learning between repeated cocaine administration and a cocaine-paired chamber. Two weeks after the viral injection into the NAc, the CPP test was conducted by administering cocaine at one fixed chamber and saline at the other chamber for 3 d. On day 4, place preference to visit the cocaine-paired chamber was determined without administration of cocaine (Fig. 1*B*). As reported previously (14), bilateral blockade of the direct pathway, but not that of the indirect pathway, significantly reduced the cocaine-induced CPP. In the control, infusion of saline into the intact side of the NAc of the D-aRNB or I-aRNB mice showed unchanged cocaine-induced CPP, comparable to that of cocaine-administered, saline-injected WT mice (Fig. 1*B*). This finding verified that blockade of one side of transmission had no effect on cocaine sensitization. Then, the regulation of acquisition of cocaine-induced adaptation by DA receptors was examined by drug infusion 20 min before each cocaine administration (Fig. 1*B*). When a D1 antagonist was infused into the D-aRNB mice, they showed a significant reduction in CPP, similar to that of the bilaterally blocked D-RNB mice. In contrast, infusion of a D1 agonist, a D2 agonist, or a D2 antagonist in the D-aRNB mice showed no such reduction in the cocaine-induced CPP. Furthermore, none of the DA agents prevented the cocaine-induced CPP in either the virus-transfected WT mice or the I-aRNB ones (Fig. 1*B*). As controls, no alteration of locomotion activity was observed in both D-aRNB and I-aRNB mice after treatments with DA agonists and antagonists (17). These results indicated that activation of D1 receptors in the direct pathway is critical for inducing cocaine sensitization.

Next, we addressed whether DA receptors could be involved in the expression of cocaine sensitization once such sensitization had been developed by repeated cocaine administration (Fig. 1*C*). In this test, animals were conditioned by daily administration of cocaine for 3 d. On day 4, saline or a DA agent was injected into the intact side of the NAc; 20 min later, the CPP test was conducted without cocaine administration. The D1 antagonist markedly prevented expression of CPP in the D-aRNB mice, and this prevention was not only D1 receptor antagonist-selective but also direct pathway–specific (Fig. 1*C*). These results demonstrated that the activation of D1 receptors in the direct pathway is necessary for both acquisition and expression of cocaine-induced addictive behavior.

D1 Receptor Regulation of the Direct Pathway in Acquisition of Appetitive Reward Learning. Regulation of DA receptors in acquisition and expression of appetitive reward learning was examined by measuring CPP of palatable chocolate over the standard food with the same procedures used for CPP of cocaine administration (Fig. 2). Bilateral blockade of the direct pathway, but not the indirect pathway, markedly impaired appetitive reward learning (14) (Fig. 2*A*). In contrast, unilaterally blocked, saline-infused D-aRNB or I-aRNB mice showed normal ability to learn a chocolate-paired chamber in the CPP test. Then, when a specific DA agonist or antagonist was injected into the intact side of the NAc 20 min before each conditioning with chocolate, the D1 antagonist-treated D-aRNB mice were severely impaired in acquisition of appetitive reward learning (Fig. 2*A*). This impairment was selective for D1 receptors in the direct pathway;

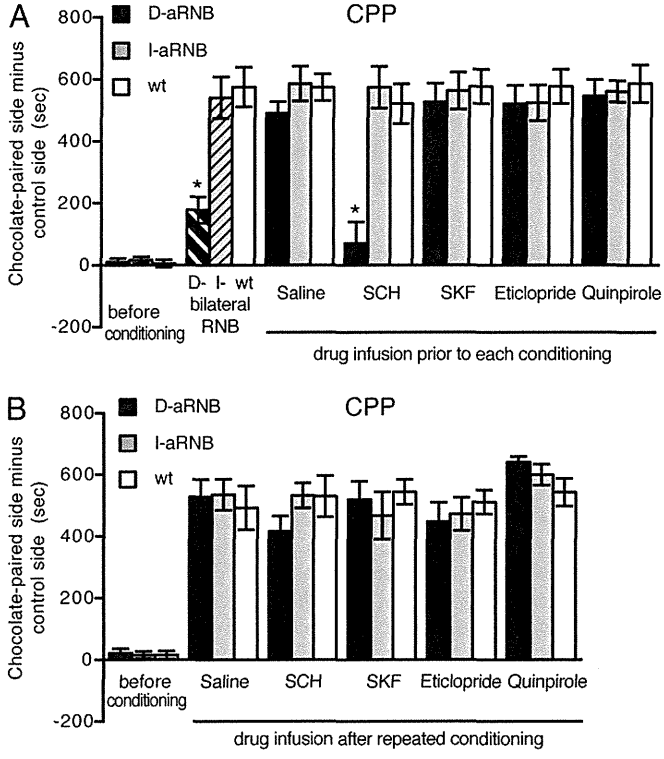

Fig. 2. Acquisition but not expression of appetitive reward learning by D1 receptor activation in the direct pathway. (*A*) Saline or the indicated DA agent was injected into the NAc 20 min before conditioning of mice with chocolate at one fixed chamber and a standard food at the other chamber. This conditioning was repeated for 3 d, and CPP was tested on day 4 without injection of saline or the DA agent (n = 5–6). (*B*) Mice were place-conditioned with chocolate for 3 d. On day 4, saline or the indicated DA agent was injected; 20 min later, CPP was tested (n = 5–6). Columns and bars represent the mean ± SEM, respectively. D-RNB vs. I-RNB/WT or D-aRNB vs. I-aRNB/WT, $*P < 0.05$.

none of the other groups of drug-infused animals were defective in acquisition of appetitive reward learning (Fig. 2*A*). Notably, once the D-aRNB mice had learned a reward by repeated appetitive conditioning for 3 d, infusion of the D1 antagonist failed to abrogate appetitive reward learning (Fig. 2*B*). Also, none of the other groups of drug-infused animals showed impaired expression of appetitive reward learning (Fig. 2*B*). These results indicated that the activation of D1 receptors in the direct pathway is essential for acquisition of appetitive reward learning but is not required for expression of this learning behavior.

D2 Receptor Dependency of the Indirect Pathway in Aversive Behavior. Aversive learning was then tested by performing the one-trial inhibitory avoidance task (Fig. 3). In this test, mice received electric shocks when they entered a preferred dark chamber from a lighted chamber. Aversive behavior was then tested 24 h later by measuring latencies to enter the dark chamber, where the mice were electrically shocked (14). In the absence of aversive conditioning, all three groups of animals (WT, D-aRNB, and I-aRNB) rapidly entered the preferred dark chamber with no statistical difference regardless of infusion of DA receptor agonists or antagonists. Then, bilateral blockade, but not unilateral blockade, of the indirect pathway impaired aversive learning to avoid entering the electrically shocked chamber (Fig. 3*A*). When quinpirole or aripiprazole was infused into the NAc 20 min before aversive conditioning, either of these D2 agonists effectively impaired avoidance learning of the I-aRNB mice but not that of the D-aRNB or WT mice (Fig. 3*A*). No such impairment was elicited by infusion of the D1 agonist, D1 antagonist, or D2 antagonist into the I-aRNB mice or by infusion of any of the DA agents into the WT or D-aRNB mice (Fig. 3*A*).

The effects of DA agents on the expression of avoidance learning were then tested (Fig. 3*B*). Animals were conditioned with electric shocks in the dark chamber and subsequently kept in their home cage for 24 h. DA agents were then infused into the NAc; 20 min later, the animals were tested for their ability to avoid the electrically shocked chamber. This analysis showed selective impairments of aversive behavior by the activation of the D2 receptor with its agonists, quinpirole and aripiprazole, only in the I-aRNB mice (Fig. 3*B*). The results thus indicated that the inactivation of D2 receptors in the indirect pathway is indispensable for both acquisition and expression of aversive behavior.

Critical Function of Postsynaptic D2L Receptors in Aversive Behavior. In the expression of D2 receptors, a short form (D2S) and a long form (D2L) of D2 receptors are generated by the respective exclusion and inclusion of a 29-amino acid sequence in the third cytoplasmic domain of the D2 receptors via alternative splicing (18–20). The D2L receptors have been shown to be responsible for DA transmission at the postsynaptic site of striatal neurons (21, 22). We thus addressed whether the observed aversive

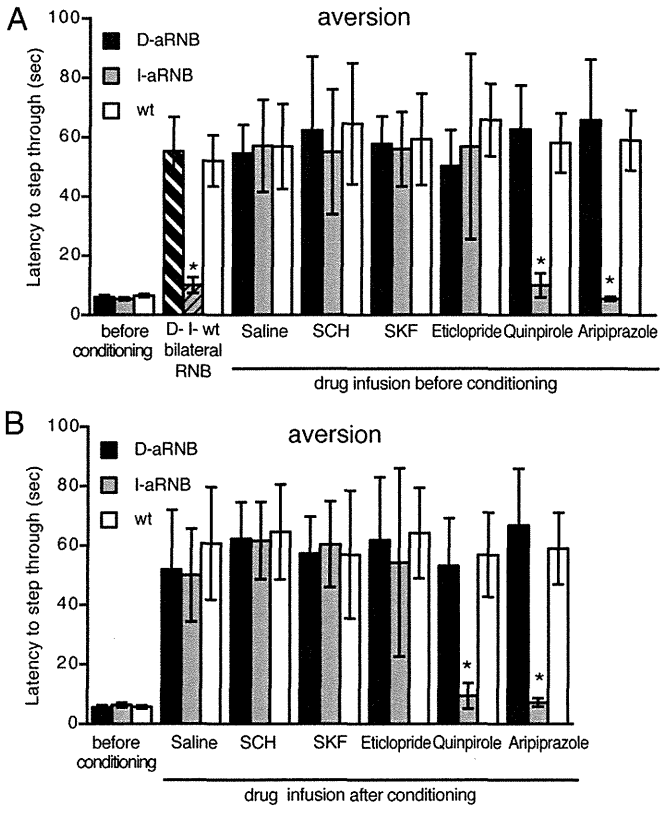

Fig. 3. Acquisition and expression of aversive learning by D2 receptor inactivation in the indirect pathway. (*A*) Aversive learning was tested by the one-trial inhibitory avoidance task. Saline or the indicated DA agent was injected into the NAc; 20 min later, the mice were subjected to electric shocks when they entered the dark chamber from the lighted chamber. Memory retention was tested 24 h later by measuring latencies for the mice to enter the dark chamber (n = 5–6). (*B*) Mice were conditioned with electric shocks at the dark chamber; 24 h later, saline or the indicated DA agent was injected. Twenty minutes later, latencies to enter the dark chamber were measured (n = 4–6). Columns and bars represent the mean ± SEM, respectively. I-RNB vs. D-RNB/WT or I-aRNB vs. D-aRNB/WT, $*P < 0.05$.

learning was mediated by the postsynaptic D2 receptors in DA transmission of the striatal neurons by examining aversive behavior of D2L knockout mice (23). Upon one-trial inhibitory avoidance analysis, the D2L knockout mice showed significant impairment in aversive learning in a gene dosage–dependent manner (Fig. 4*A*). This deficit was not due to impairments of the fear system, because the three groups of animals (WT, $D2L^{+/-}$, and $D2L^{-/-}$ mice) showed comparable postshock freezing responses by repeated presentation of footshocks (Fig. 4*B*). These data thus indicated that the postsynaptic D2 receptors are critical for regulating DA transmission in aversive behavior.

Involvement of Additional Key Neurotransmitter Receptors in Aversive Learning. The inactivation of the inhibitory D2 receptors would most likely enhance the efficacy of input transmission of aversive stimuli in the indirect pathway and would thus induce aversive learning. The induction of LTP in glutamatergic transmission in the indirect-pathway neurons has been reported based on extensive electrophysiological studies using striatal slice preparations (10, 11, 24). In the indirect-pathway neurons, D2 receptors and adenosine A2a receptors are colocalized postsynaptically and counteract each other (10, 24, 25). The activation of postsynaptic A2a receptors efficiently impedes the synthesis of endocannabinoids and results in suppression of the presynaptic CB1 receptors in glutamatergic neurons through reduced retrograde transmission of endocannabinoids (13, 25). Electrophysiological studies have indicated that when the D2 receptors in the indirect-pathway neurons are inhibited or the striatal DA levels are reduced, the NMDA receptors and A2a receptors are coactivated and that elaborate synaptic modulation via the NMDA, A2a, and CB1 receptors induces LTP in glutamatergic transmission in the indirect-pathway neurons (10–12). Therefore, we examined whether these key neurotransmitter receptors could be involved in aversive learning by infusing the inhibitors or activator of these respective receptors into the intact side of the NAc of the I-aRNB mice. When a mixture of NMDA receptor inhibitors, D-(-)-2-amino-5-phosphonovalerate (APV) and MK801, was unilaterally injected into the NAc, an abnormal ipsilateral rotation was evoked in both the I-aRNB mice and WT mice, but this abnormality gradually disappeared thereafter. No such abnormal turning was detected when the A2a receptor antagonist SCH58261 or the CB1 receptor agonist arachidonyl-2-chloroethylamide (ACEA) was injected into the NAc of the I-aRNB and WT mice. Notably, the drug-treated, unconditioned I-aRNB and WT mice still retained preference to step through from the lighted chamber to the preferred dark chamber with no statistical difference between these two groups (Fig. 5). Then, 20 min after drug injection, the animals were conditioned with electric shocks in the dark chamber, and retention of aversive learning was tested 24 h after electric shocks by performing the one-trial inhibitory avoidance task. Treatments with the NMDA receptor inhibitors abolished aversive learning of the I-aRNB mice, but not that of the WT mice (Fig. 5*A*). Similarly, infusion of the A2a receptor antagonist SCH58261 significantly impaired the aversive learning of the I-aRNB mice compared with that of the WT mice (Fig. 5*B*). Furthermore, treatments with the CB1 receptor agonist ACEA hampered the aversive learning of the I-aRNB mice only (Fig. 5*C*). These results thus indicated that aversive learning behavior is regulated by the neural plasticity involving the elaborate actions of the postsynaptic NMDA receptors and A2a receptors and the presynaptic CB1 receptors at the glutamatergic synapses of the indirect-pathway neurons.

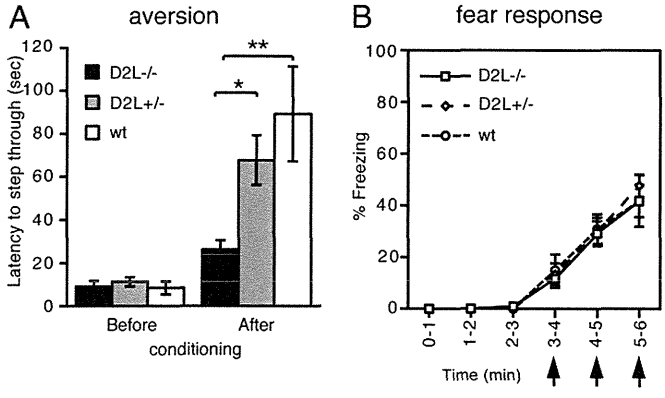

Fig. 4. Impaired aversive learning in the D2L knockout mice. (*A*) Latencies for mice to enter the dark chamber from the lighted chamber were measured before and 24 h after conditioning with electric shocks at the dark chamber. $n = 6$ for $D2L^{-/-}$ mice, 8 for $D2L^{+/-}$ mice, and 5 for WT mice. Columns and bars represent the mean ± SEM, respectively. $*P < 0.05$, $**P < 0.01$. (*B*) Percentages of freezing were determined for a 1-min period by giving electric shocks at 3, 4, and 5 min (arrows) ($n = 4$ each). Symbols and bars represent the mean ± SEM, respectively. ANOVA with repeated measures among the three groups of mice; for genotype, $P = 0.90$; for time, $P < 0.001$; interaction genotype × time, $P = 0.94$.

Discussion

This study aimed at exploring the regulatory mechanisms of the NAc circuit in reward and aversive learning by combining the pathway-specific blockade of the NAc transmission and pharmacological analysis. Learning deficits in the D1 antagonist–treated D-aRNB mice and the D2 agonist–treated I-aRNB mice both faithfully reflected those in the bilaterally blocked D- and I-RNB mice, respectively. The activation of D1 receptors in the direct pathway and the inactivation of D2 receptors in the indirect pathway are thus essential for reward-based learning and aversive learning, respectively. The present study further revealed that the postsynaptic D2 receptors serve as a prerequisite determinant that modulates a set of the LTP-evoking synaptic receptors (NMDA, A2a, and CB1 receptors) for induction of aversive learning. The NAc comprises a minor cell population of cholinergic and GABAergic interneurons that express D1-like or D2-like DA receptors and NMDA receptors (11). Pharmacological treatments in the aRNB mice may thus act on some of these interneurons and could influence the activity of the direct-pathway or indirect-pathway neurons (26, 27). The mechanisms underlying the distinct role of each pathway thus need to be carefully interpreted. The present study has demonstrated that not only the pathway-specific postsynaptic D1 and D2 receptors but also several key receptors characteristic of the corticostriatal synapses play a pivotal role in the associative reward-based and aversive learning (10–12). We thus propose a mechanistic model for reward and aversive learning by focusing on the transmission modulation of the corticostriatal synapses in the NAc (Fig. 6).

Rewarding stimuli elicit a burst of phasic firings in DA neurons (28), and these stimuli as well as cocaine administration vastly increase synaptic concentrations of DA in the NAc (29, 30). This increase effectively activates the low-affinity D1 receptors and results in induction of LTP in striatonigral neurons of the direct pathway (10, 11, 31). The simultaneous activation of the high-affinity, inhibitory D2 receptors, however, keeps the indirect pathway inactive. The D1 receptor antagonist thus disrupted cocaine-induced and reward-based behavior in a direct pathway–specific manner (Fig. 6*A*).

An electric footshock has been shown to inhibit about 90% of DA neurons in the VTA (32) and would reduce DA levels in the NAc. This reduction in DA relieves the inhibitory actions of the high-affinity D2 receptors but has no effects on the low-affinity D1 receptors. The resultant selective transmission enhancement in the indirect pathway would induce aversive learning. The exogenously applied D2 receptor agonist thus counteracted the